

Candidates for Universal Measures of Multipartite Entanglement

Samuel R. Hedemann

P.O. Box 72, Freeland, MD 21053, USA

(Dated: September 18, 2018)

We propose and examine several candidates for universal multipartite entanglement measures. The most promising candidate for applications needing entanglement in the full Hilbert space is the ent-concurrence, which detects all entanglement correlations while distinguishing between different types of distinctly multipartite entanglement, and simplifies to the concurrence for two-qubit mixed states. For applications where subsystems need internal entanglement, we develop the absolute ent-concurrence which detects the entanglement in the reduced states as well as the full state.

I. INTRODUCTION

Entanglement [1, 2], in the simplest case of pure quantum states, is when a state such as $|\psi\rangle = a|1\rangle\otimes|1\rangle + b|1\rangle\otimes|2\rangle + c|2\rangle\otimes|1\rangle + d|2\rangle\otimes|2\rangle$, where $|a|^2 + |b|^2 + |c|^2 + |d|^2 = 1$, cannot be factored as a tensor product of pure states such as $|\psi\rangle = (w|1\rangle + x|2\rangle) \otimes (y|1\rangle + z|2\rangle)$, where $|w|^2 + |x|^2 = 1$ and $|y|^2 + |z|^2 = 1$, where we have expressed each qubit in a generic basis $\{|1\rangle, |2\rangle\}$ (our convention in this paper, and these kets do not imply Fock states [3]).

Quantum mixed states are $\rho \equiv \sum_j p_j |\psi_j\rangle\langle\psi_j|$, where $p_j \in [0, 1]$, $\sum_j p_j = 1$, and all $|\psi_j\rangle$ are pure. For *bipartite* systems, those composed of two subsystems (modes), mixed states $\varsigma \equiv \varsigma^{(1,2)}$ are separable *if and only iff* (iff)

$$\varsigma^{(1,2)} = \sum_j p_j \varsigma_j^{(1)} \otimes \varsigma_j^{(2)}, \quad (1)$$

where parenthetical superscripts are mode labels, and each $\varsigma_j^{(m)}$ is pure. Each mode- m reduced state $\zeta^{(m)} \equiv \text{tr}_{\bar{m}}(\varsigma)$, where \bar{m} means “not m ” (see App. A), admits a decomposition of the form $\zeta^{(m)} \equiv \sum_j p_j \zeta_j^{(m)} = \sum_j p_j \varsigma_j^{(m)}$ as proved in App. B, so if we only knew reductions $\zeta^{(m)}$, we could search decompositions of each one to find the pair with matching sets $\{p_j\}$ such that $\varsigma^{(1,2)} = \sum_j p_j \zeta_j^{(1)} \otimes \zeta_j^{(2)}$. Therefore knowledge of the reductions allows reconstruction of the *parent state* ς .

For N -partite (N -mode) systems, *separability can occur in more than one way*. For example, two different 3-qubit pure states could have *separable bipartitions* as $\rho = \check{\rho}^{(1)} \otimes \check{\rho}^{(2,3)}$ and $\varrho = \check{\varrho}^{(1,2)} \otimes \check{\varrho}^{(3)}$, so we call *both* of them *biseparable* or *2-separable*, even though the mode groups that are separable for each state are different.

These different mode-groupings are called *partitions*, which are definitions of *new modes* composed of (but not subdividing) the original modes m_k , as explained in App. C. For example, a tripartite state like $\rho^{(1,2,3)}$ can have three unique bipartitions $\rho^{(1|2,3)}, \rho^{(2|1,3)}, \rho^{(3|1,2)}$ and one unique tripartition $\rho^{(1|2|3)} = \rho^{(1,2,3)}$, showing that in the absence of partitions, the commas *are* the partitions.

To handle the general N -partite phenomenon of separability of a given partitioning having the potential to occur in different ways, the notion of k -separability was developed [4–17], as depicted in Fig. 1.

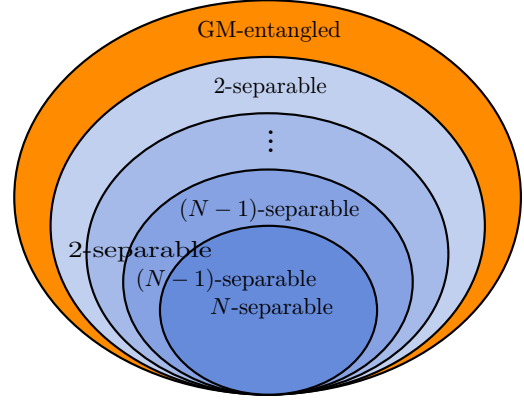


FIG. 1: (color online) Relationships of k -separabilities [4]. Each k -separability implies all lower- k -separabilities, and is necessary for all higher- k -separabilities. Thus, N -separable states are *also* $(N-1)$ -separable, all the way down to 2-separable, but some 2-separable states are not 3-separable or higher. The “1-separable” states are “genuinely multipartite (GM) entangled,” also defined as all states that are not 2-separable. Thus, *the GM-entangled region is strictly crescent-shaped here*, while *the k -separable regions are each ellipse-shaped and coinciding with parts of all lower- k -separabilities*. (The shapes are arbitrary, merely representing relationships.)

By definition, k -separability of *pure* states is when *any* member of the set of all possible k -partitions has k -mode product form, for a fixed k . Thus, for a pure $\rho^{(1,2,3)}$, if only $\rho^{(2|1,3)}$ is 2-separable, but not $\rho^{(1|2,3)}$ or $\rho^{(3|1,2)}$, then that is sufficient for $\rho^{(1,2,3)}$ to be 2-separable.

Mixed states are k -separable if a decomposition exists for which all pure decomposition states are *at least* k -separable, with one being exactly k -separable [4] (since higher-than- k -separabilities are also k -separable, we can just say that all decomposition states need to be k -separable). For example, the 3-qudit state

$$\rho = \sum_j p_j \rho_j^{(1)} \otimes \rho_j^{(2,3)} + \sum_k q_k \rho_k^{(2)} \otimes \rho_k^{(1,3)} + \sum_l r_l \rho_l^{(3)} \otimes \rho_l^{(1,2)}, \quad (2)$$

where $p_j, q_k, r_l \in [0, 1]$, $(\sum_j p_j) + (\sum_k q_k) + (\sum_l r_l) = 1$, with pure entangled bipartite states $\rho_j^{(2,3)}, \rho_k^{(1,3)}, \rho_l^{(1,2)}$ and pure $\rho_j^{(1)}, \rho_k^{(2)}, \rho_l^{(3)}$, is *2-separable (biseparable)*, even though each group of pure decomposition states is separable over *different* bipartitions [4].

Here, we define the “absence of k -separability” (meaning no k -partitions of a pure state have k -partite product form) as *full k -partite entanglement* (F_k -entanglement) for $k > 1$ as shown in Fig. 2, found by *combining* entanglement values (by some measure) over all k -partitions, and named in analogy to “full N -partite entanglement” being the absence of full N -partite separability. However, the absence of 2-separability is *also* “2-entanglement,” known as “genuinely multipartite (GM) entanglement.” We use the term *GM- k -entanglement* (GM_k -entanglement) in lieu of the traditional term “ k -entanglement” as the minimum entanglement over all k -partitions.

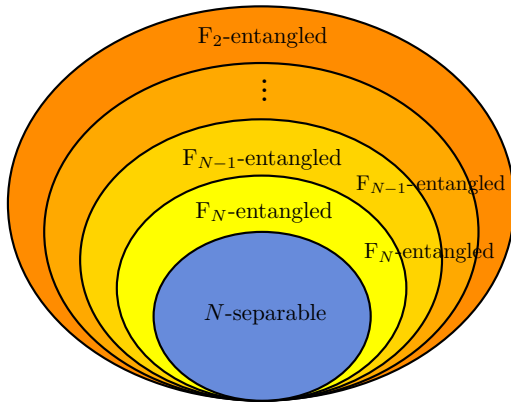


FIG. 2: (color online) Relationships of F_k -entanglements. Here, a given F_k -entanglement implies all higher- k F_k -entanglements, while being itself necessary for all lower- k F_k -entanglements. Thus, *each F_k -entanglement region is strictly crescent-shaped and coinciding with parts of all higher- k F_k -entanglements*, with F_N -entanglement being the thickest crescent, and all lower- k F_k -entanglements having progressively thinner crescents. The entire region that is not N -separable is F_N -entangled.

On the other hand, N -partite states are entangled iff they are F_N -entangled, as proved in App. D. This means that the complete absence of entanglement correlations can only occur in N -partite states that are N -separable, meaning states with an *optimal decomposition*,

$$\zeta^{(1,\dots,N)} = \sum_j p_j \bigotimes_{m=1}^N \zeta_j^{(m)} = \sum_j p_j \zeta_j^{(1)} \otimes \dots \otimes \zeta_j^{(N)}, \quad (3)$$

where the $\zeta_j^{(m)}$ are pure. N -partite states that *cannot* be expanded as (3) are *full N -partite entangled* (F_N -entangled). We will often say *entanglement correlation* instead of just *entanglement* to remind that there are *other* kinds of nonlocal correlation not involving entanglement.

However, F_N -entanglement cannot distinguish between types of multipartite entanglement. For example, given

$$\rho_{|\Phi_{\text{GHZ}}\rangle} \quad \text{and} \quad \rho_{|\Phi_{\text{BP}}\rangle} \equiv \rho_{|\Phi^+\rangle} \otimes \rho_{|\Phi^+\rangle}, \quad (4)$$

where $|\Phi_{\text{GHZ}}\rangle \equiv \frac{1}{\sqrt{2}}(|1,1,1,1\rangle + |2,2,2,2\rangle)$ is a 4-qubit GHZ state [18–20] where $\rho_{|A\rangle} \equiv |A\rangle\langle A|$, and $|\Phi^+\rangle \equiv \frac{1}{\sqrt{2}}(|1,1\rangle + |2,2\rangle)$ is a 2-qubit Bell state so that $\rho_{|\Phi_{\text{BP}}\rangle}$ is a “Bell-product state,” since both $\rho_{|\Phi_{\text{GHZ}}\rangle}$ and $\rho_{|\Phi_{\text{BP}}\rangle}$ have maximal mixing in all single-mode reductions, an F_N -entanglement measure would report both states as being equally entangled, despite $\rho_{|\Phi_{\text{GHZ}}\rangle}$ being F_2 -entangled and GM_2 -entangled while $\rho_{|\Phi_{\text{BP}}\rangle}$ is 2-separable.

Yet, GM_2 -entanglement alone cannot detect the strong entanglement correlations within the Bell states of $\rho_{|\Phi_{\text{BP}}\rangle}$ in (4). Thus, while F_N -entanglement can detect the presence of all entanglement correlations but cannot distinguish k -separabilities, lone sub- N GM_k -entanglement measures are not sufficient to detect the presence of all entanglement correlations, but *can* verify k -separability.

Therefore our main goal here is to define a few candidate universal entanglement measures that distinguish between types of multipartite entanglement without discarding information about entanglement correlations, which individual GM_k -entanglement measures cannot do alone.

The building-block of our candidate measures is the F_N -entanglement measure *the ent* [21], given by

$$\Upsilon(\rho) \equiv \Upsilon(\rho, \mathbf{n}) \equiv \frac{1}{M(L_*)} \left(1 - \frac{1}{N} \sum_{m=1}^N \frac{n_m P(\check{\rho}^{(m)}) - 1}{n_m - 1} \right), \quad (5)$$

for pure states ρ of an N -mode n -level system where mode m has n_m levels and $\mathbf{n} \equiv (n_1, \dots, n_N)$, so that $n = n_1 \dots n_N = \det(\text{diag}(\mathbf{n}))$, $N = \dim(\mathbf{n})$, $P(\sigma) \equiv \text{tr}(\sigma^2)$ is the purity of σ , and $\check{\rho}^{(m)}$ is the n_m -level single-mode reduction of ρ for mode m (see App. A). The normalization factor $M(L_*) \equiv M(L_*, \mathbf{n})$ is given in App. E. Basically, the ent measures how simultaneously mixed the $\check{\rho}^{(m)}$ are.

We will also use the *partitional ent* $\Upsilon^{(\mathbf{m}^{(T)})}(\rho) \equiv \Upsilon(\check{\rho}^{(\mathbf{m})}, \mathbf{n}^{(\mathbf{m}^{(T)})})$, allowing us to repartition ρ 's reduction $\check{\rho}^{(\mathbf{m})}$ (including the nonreduction $\check{\rho}^{(\mathbf{N})} \equiv \check{\rho}^{(1,\dots,N)} = \rho$) into new mode groups $\mathbf{m}^{(T)} \equiv (\mathbf{m}^{(1)} | \dots | \mathbf{m}^{(T)})$ of levels $\mathbf{n}^{(\mathbf{m}^{(T)})} \equiv (n_{\mathbf{m}^{(1)}}, \dots, n_{\mathbf{m}^{(T)}})$ (see App. C) to measure the F_T -entanglement of any T mode groups (see [21] for details). Finally, when ρ or $\check{\rho}^{(\mathbf{m})}$ are *mixed*, we use convex-roof extensions as $\hat{\Upsilon}$ and $\hat{\Upsilon}^{(\mathbf{m}^{(T)})}$ (see [21, App. J]), which are minimum average ents over all decompositions. The main sections of this paper are:

I.	Introduction	1
II.	Candidate Pure-State Entanglement Measures	3
III.	Tests of Candidate Pure-State Measures	3
IV.	Candidate Mixed-State Measures	6
V.	Tests of Candidate Mixed-State Measures	6
VI.	Ent-Concurrence	8
VII.	Absolute Ent-Concurrence	9
VIII.	Conclusions	11
App.	Appendices	12
A.	Brief Review of Reduced States	12
B.	N-Separability of N-Partite States Implies Reconstructability by Smallest Reductions	12
C.	Definition of Partitions	12
D.	Proof that N-Partite States are Entangled If and Only If they are F_N-Entangled	13
E.	Normalization Factor of the Ent	14
F.	True-Generalized X (TGX) States	15
G.	Full Set of 4-Qubit Maximally F_N-Entangled TGX States Involving $1\rangle$	15
H.	Quantum Mixed States Cannot Be Treated as Time-Averages of Varying Pure States	15

and wherever possible, details are put in the Appendices.

II. CANDIDATE PURE-STATE ENTANGLEMENT MEASURES

Here we introduce the candidate entanglement measures under consideration. Each will use the ent from (5) as well as its various different forms due to partitioning. See [21] for full explanations. We start with *pure*-state measures, and discuss mixed input after initial tests.

A. Full Genuinely Multipartite (FGM) Ent

The FGM ent for pure ρ is

$$\Upsilon_{\text{FGM}}(\rho) \equiv \frac{1}{M_{\text{FGM}}} \sum_{k=2}^N \Upsilon_{\text{GM}_k}(\rho), \quad (6)$$

where M_{FGM} is a normalization factor, and

$$\Upsilon_{\text{GM}_k}(\rho) \equiv \min(\{\Upsilon^{(\mathbf{N}_h^{(k)})}(\rho)\}), \quad (7)$$

which is the GM_k ent, where $\{\Upsilon^{(\mathbf{N}_h^{(k)})}(\rho)\}$ is the set of all N -mode k -partitional ents, each labeled by h . Note that [21] defined the *GM ent* as $\Upsilon_{\text{GM}}(\rho) \equiv \Upsilon_{\text{GM}_2}(\rho)$, which is the “ent-version” of GM concurrence $C_{\text{GM}}(\rho)$ [5].

Since Υ_{FGM} sums all GM_k ents, it is a measure of *simultaneous* GM_k -entanglements; that is, it rates states for which the *combination* of all their GM_k -entanglements is maximal as being “maximally FGM-entangled.”

B. Full Simultaneously Multipartite (FSM) Ent

The FSM ent for pure ρ is

$$\Upsilon_{\text{FSM}}(\rho) \equiv \frac{1}{M_{\text{FSM}}} \sum_{k=2}^N \Upsilon_{\text{SM}_k}(\rho), \quad (8)$$

where M_{FSM} is a normalization factor, and we define the *simultaneously multipartite k -ent* (SM_k ent) as

$$\Upsilon_{\text{SM}_k}(\rho) \equiv \frac{1}{M_{\text{SM}_k}} \sum_{h=1}^{\{N_k\}} \Upsilon^{(\mathbf{N}_h^{(k)})}(\rho), \quad (9)$$

where $\{N_k\} \equiv \frac{1}{k!} \sum_{j=0}^k (-1)^{k-j} \binom{k}{j} j^N$ are Stirling numbers of the second kind, $\binom{k}{j} \equiv \frac{k!}{j!(k-j)!}$, $\{\Upsilon^{(\mathbf{N}_h^{(k)})}(\rho)\}$ is the set of all N -mode k -partitional ents, and M_{SM_k} is a normalization factor. $\Upsilon_{\text{SM}_k}(\rho)$ detects the presence of *any* entanglement correlation among *all* possible k -partitions of ρ . Thus, it cannot ignore entanglement within particular k -partitions just because a different k -partition is separable as $\Upsilon_{\text{GM}_k}(\rho)$ can.

The FSM ent Υ_{FSM} is a measure of *simultaneous* SM_k ents; which means it is a measure of the combination of *all* N -mode partitional ents, so it is a sum of all 2-partitional ents of ρ , all 3-partitional ents of ρ , all the way up to the N -partitional ent (the ent itself). Thus, if there is *any* entanglement correlation between *any* mode groups of ρ , the FSM will detect it, and states that maximize it are “maximally FSM-entangled.”

C. Full Distinguishably Multipartite (FDM) Ent: The Ent-Concurrence

The FDM ent (or the *ent-concurrence*) for pure ρ is

$$\Upsilon_{\text{FDM}}(\rho) \equiv \frac{1}{M_{\text{FDM}}} \sum_{k=2}^N \Upsilon_{\text{DM}_k}(\rho), \quad (10)$$

where M_{FDM} is a normalization factor, and we define the *distinguishably multipartite k -ent* (DM_k ent) as

$$\Upsilon_{\text{DM}_k}(\rho) \equiv \frac{1}{M_{\text{DM}_k}} \sum_{h=1}^{\{N_k\}} \sqrt{\Upsilon^{(\mathbf{N}_h^{(k)})}(\rho)}, \quad (11)$$

where M_{DM_k} is a normalization factor, $\{N_k\}$ are Stirling numbers of the second kind as in (9), and $\{\Upsilon^{(\mathbf{N}_h^{(k)})}(\rho)\}$ is the set of all N -mode k -partitional ents.

The FDM ent Υ_{FDM} is a measure of simultaneous DM_k ents Υ_{DM_k} , and the Υ_{DM_k} measures not only the combination of all possible N -mode k -partitional ents, but also *how equally distributed* they are, rating states for which all N -mode k -partitional ents have the highest combination and are the most equal and numerous as having the highest DM_k ent.

This is based on *pseudonorm* $|\mathbf{x}|_{1/2} \equiv \sum_k \sqrt{x_k}$; $x_k \geq 0$, which obeys $|\mathbf{x}|_{1/2} = 0 \Rightarrow \mathbf{x} = \mathbf{0}$ and the triangle inequality, and although $|\mathbf{ax}|_{1/2} \neq |a| \cdot |\mathbf{x}|_{1/2}$, that does not matter here, since our “vectors” are really just lists of scalars. The main reason we use this pseudonorm is because it rates an equally distributed 1-norm-normalized vector such as $\mathbf{x} = (0.25, 0.25, 0.25, 0.25)$ as having the *highest* “ $\frac{1}{2}$ -norm” value out of all vectors of the same 1-norm, such as $\mathbf{y} = (0, 0, 0.5, 0.5)$ or $\mathbf{z} = (0, 1, 0, 0)$.

For two qubits ($N = 2$), the FDM ent is the *concurrence* C [22, 23], since $\Upsilon = C^2$ as proven in [21], so that

$$\Upsilon_{\text{FDM}}(\rho) = \Upsilon_{\text{DM}_N}(\rho) = \sqrt{\Upsilon(\rho)} = C(\rho), \quad (12)$$

(extendible to mixed states, as shown later). Therefore, if we let the *N -mode k -partitional ent-concurrence* be

$$C_{\Upsilon}^{(\mathbf{N}_h^{(k)})}(\rho) \equiv \sqrt{\Upsilon^{(\mathbf{N}_h^{(k)})}(\rho)}, \quad (13)$$

where $\{\Upsilon^{(\mathbf{N}_h^{(k)})}(\rho)\}$ is the set of all N -mode k -partitional ents, then the DM_k ent Υ_{DM_k} is simply a 1-norm of all $\{C_{\Upsilon}^{(\mathbf{N}_h^{(k)})}(\rho)\}$ for a given k . Therefore, the Υ_{FDM} in (10) can also be called the *ent-concurrence* C_{Υ} for pure states.

III. TESTS OF CANDIDATE PURE-STATE MEASURES

For simple tests, we use 4-qubit ($2 \times 2 \times 2 \times 2$) states,

$$\begin{aligned} |\Phi_{\text{GHZ}}\rangle &\equiv \frac{1}{\sqrt{2}}(|1,1,1,1\rangle + |2,2,2,2\rangle) \\ |\Phi_{\text{BP}}\rangle &\equiv \frac{1}{\sqrt{4}}(|1,1,1,1\rangle + |1,1,2,2\rangle + |2,2,1,1\rangle + |2,2,2,2\rangle) \\ |\Phi_{\text{F}}\rangle &\equiv \frac{1}{\sqrt{4}}(|1,1,1,1\rangle + |1,1,2,2\rangle + |2,2,1,2\rangle + |2,2,2,1\rangle) \\ |\psi_{\text{W}}\rangle &\equiv \frac{1}{\sqrt{4}}(|1,1,1,2\rangle + |1,1,2,1\rangle + |1,2,1,1\rangle + |2,1,1,1\rangle) \\ |\psi_{\text{Rand}}\rangle &\equiv \sum_{k=1}^{16} a_k |k\rangle; \quad \sum_{k=1}^{16} |a_k|^2 = 1, \end{aligned} \quad (14)$$

where $|\Phi_{\text{BP}}\rangle \equiv |\Phi^+\rangle \otimes |\Phi^+\rangle$ is the Bell product from (4), $|\psi_{\text{W}}\rangle$ is the W state [24], and $|\psi_{\text{Rand}}\rangle$ is a random 16-level pure state, where here and throughout we use basis abbreviation $\{|1\rangle, |2\rangle, \dots, |n\rangle\} \equiv \{|1,1,1,1\rangle, |1,1,1,2\rangle, \dots, |2,2,2,2\rangle\}$. The states $|\Phi_{\text{GHZ}}\rangle$, $|\Phi_{\text{BP}}\rangle$, and $|\Phi_{\text{F}}\rangle$ are taken from the set of maximally F_N -entangled true-generalized X (TGX) states (see App. F, [21, App. D], and [25]), chosen from the subset including $|1\rangle$, generated by the 13-step algorithm of [21]. Thus, (14) provides three maximally F_N -entangled states and two other kinds of states for comparison.

The subset $\{|\Phi_{\text{GHZ}}\rangle, |\Phi_{\text{BP}}\rangle, |\Phi_{\text{F}}\rangle\}$ was chosen from the full set of F_N -entangled TGX states since they produced distinct results for the measures under test and included $|\Phi_{\text{GHZ}}\rangle$. See App. G for the full set initially used.

As an example showing the partitional ents involved, unnormalized expansion of the FGM ent in (6) is

$$\tilde{\Upsilon}_{\text{FGM}}(\rho) = \Upsilon_{\text{GM}_2} + \Upsilon_{\text{GM}_3} + \Upsilon_{\text{GM}_N}, \quad (15)$$

where $\Upsilon_{\text{GM}_2} = \min\{\Upsilon^{(1|2,3,4)}, \Upsilon^{(2|1,3,4)}, \Upsilon^{(3|1,2,4)}, \Upsilon^{(4|1,2,3)}, \Upsilon^{(1,2|3,4)}, \Upsilon^{(1,3|2,4)}, \Upsilon^{(1,4|2,3)}\}$, and $\Upsilon_{\text{GM}_3} = \min\{\Upsilon^{(1|2|3,4)}, \Upsilon^{(1|3|2,4)}, \Upsilon^{(1|4|2,3)}, \Upsilon^{(1|3|2,4)}, \Upsilon^{(1|4|2,3)}, \Upsilon^{(2|3|1,4)}, \Upsilon^{(2|4|1,3)}, \Upsilon^{(3|4|1,2)}\}$, and $\Upsilon_{\text{GM}_N} = \min\{\Upsilon^{(1|2|3|4)}\} = \Upsilon$, all using N -mode partitional ents.

A. Tests and Analysis of FGM Ent

Figure 3 explores the FGM ent of the test states in (14), with only the results for the $|\psi_{\text{Rand}}\rangle$ that had the highest unnormalized FGM ent $\tilde{\Upsilon}_{\text{FGM}}$ out of 1000 random states.

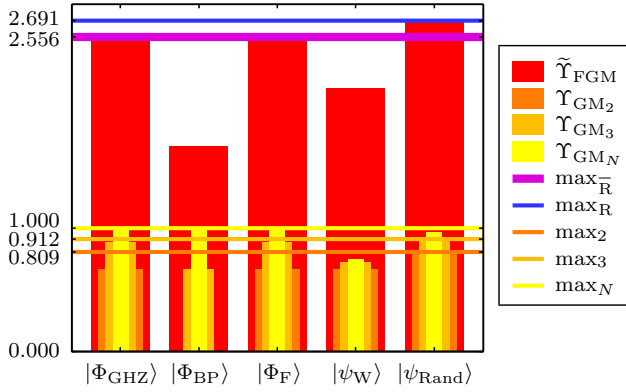


FIG. 3: (color online) Unnormalized FGM ent $\tilde{\Upsilon}_{\text{FGM}}$ of (6) for the test states of (14), with only the $|\psi_{\text{Rand}}\rangle$ that maximizes it after 1000 random pure states were tested. The normalized GM_k ents Υ_{GM_k} of (7) are also shown, and the maximum of each over all test states is $\text{max}_k \equiv \max(\Upsilon_{\text{GM}_k})$, while $\text{max}_{\bar{R}} \equiv \max(\tilde{\Upsilon}_{\text{FGM}})$ applies to all nonrandom test states, and $\text{max}_R \equiv \max(\tilde{\Upsilon}_{\text{FGM}}(\rho_{|\psi_{\text{Rand}}\rangle}))$.

As Fig. 3 shows, the maximally F_N -entangled ($N = 4$) states $|\Phi_{\text{GHZ}}\rangle$ and $|\Phi_{\text{F}}\rangle$ have identical results for all Υ_{GM_k} and $\tilde{\Upsilon}_{\text{FGM}}$, but the maximally F_N -entangled $|\Phi_{\text{BP}}\rangle$ has $\Upsilon_{\text{GM}_2} = 0$ and therefore a lower $\tilde{\Upsilon}_{\text{FGM}}$, despite matching $|\Phi_{\text{GHZ}}\rangle$ and $|\Phi_{\text{F}}\rangle$ for Υ_{GM_N} . As expected, $|\psi_{\text{W}}\rangle$ is not maximal in any quantity, but still has fairly high

values, and actually *outperforms* $|\Phi_{\text{BP}}\rangle$ in Υ_{GM_2} , Υ_{GM_3} , and $\tilde{\Upsilon}_{\text{FGM}}$, despite its lower Υ_{GM_N} .

Interestingly, $|\psi_{\text{Rand}}\rangle$ reached a *higher* $\tilde{\Upsilon}_{\text{FGM}}$ than all other test states, since its Υ_{GM_2} and Υ_{GM_3} are *higher* than those of the other states, while its Υ_{GM_N} is still slightly *lower* than 1. This proves by example that there are nonmaximally- F_N -entangled FGM-entangled states with higher $\tilde{\Upsilon}_{\text{FGM}}$ than maximally F_N -entangled states.

B. Tests and Analysis of FSM Ent

Here, Fig. 4 applies the same tests as in Fig. 3, but this time for the FSM ent of (8).

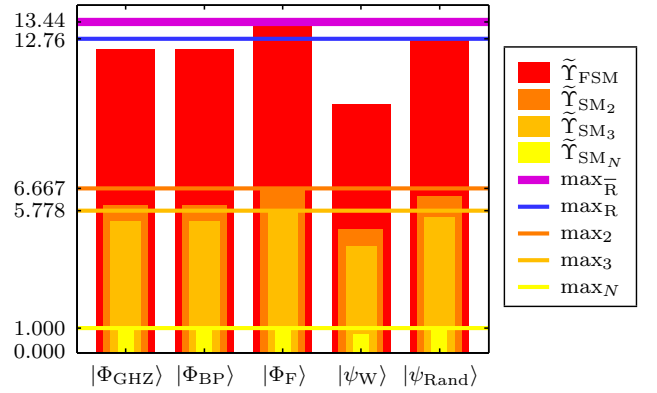


FIG. 4: (color online) Unnormalized FSM ent $\tilde{\Upsilon}_{\text{FSM}}$ of (8) for the test states of (14), with only the $|\psi_{\text{Rand}}\rangle$ that maximizes it over 1000 random pure states. The *unnormalized* SM_k ents $\tilde{\Upsilon}_{\text{SM}_k}$ of (9) are also shown, and the maximum of each over all test states is $\text{max}_k \equiv \max(\tilde{\Upsilon}_{\text{SM}_k})$, while $\text{max}_{\bar{R}} \equiv \max(\tilde{\Upsilon}_{\text{FSM}})$ applies to all nonrandom test states, and $\text{max}_R \equiv \max(\tilde{\Upsilon}_{\text{FSM}}(\rho_{|\psi_{\text{Rand}}\rangle}))$.

Here, we see that $|\Phi_{\text{BP}}\rangle$ has the *same* $\tilde{\Upsilon}_{\text{SM}_k}$ and $\tilde{\Upsilon}_{\text{FSM}}$ as $|\Phi_{\text{GHZ}}\rangle$, but that *both* $|\Phi_{\text{GHZ}}\rangle$ and $|\Phi_{\text{BP}}\rangle$ *underperform* $|\Phi_{\text{F}}\rangle$ in terms of $\tilde{\Upsilon}_{\text{SM}_2}$, $\tilde{\Upsilon}_{\text{SM}_3}$, and $\tilde{\Upsilon}_{\text{FSM}}$, despite all three states being maximally F_N -entangled. This time, $|\psi_{\text{W}}\rangle$ underperforms all other test states in every area, while $|\psi_{\text{Rand}}\rangle$ *outperforms* $|\Phi_{\text{GHZ}}\rangle$ and $|\Phi_{\text{BP}}\rangle$, while still underperforming $|\Phi_{\text{F}}\rangle$, suggesting that $|\Phi_{\text{F}}\rangle$ may be maximal in all quantities being measured.

Thus, this proves by example that some maximally F_N -entangled states are more FSM-entangled than others, even $|\Phi_{\text{GHZ}}\rangle$, and *suggests* that maximally FSM-entangled states may also be maximal for all Υ_{SM_k} .

C. Tests and Analysis of FDM Ent

Here we apply the same tests as in Sec. III A and Sec. III B, this time to the FDM ent of (10).

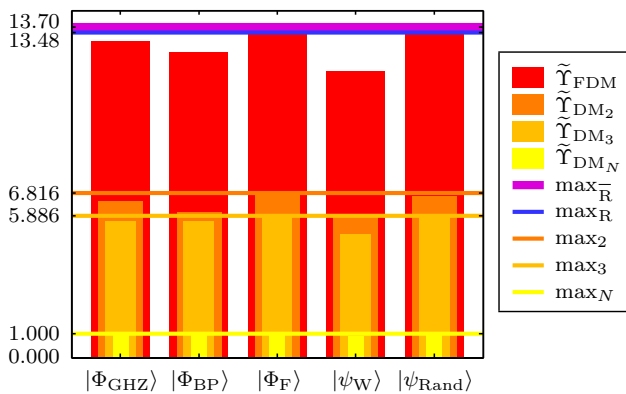


FIG. 5: (color online) Unnormalized FDM ent $\tilde{\Upsilon}_{\text{FDM}}$ (or *ent-concurrence*) of (10) for the test states of (14), with only the $|\psi_{\text{Rand}}\rangle$ that maximizes it over 1000 random pure states. The *unnormalized* DM_k ents $\tilde{\Upsilon}_{\text{DM}_k}$ of (11) are also shown, and the maximum of each over all test states is $\max_k \equiv \max(\tilde{\Upsilon}_{\text{DM}_k})$, while $\max_{\bar{R}} \equiv \max(\tilde{\Upsilon}_{\text{FDM}})$ applies to all nonrandom test states, and $\max_R \equiv \max(\tilde{\Upsilon}_{\text{FDM}}(\rho_{|\psi_{\text{Rand}}\rangle}))$.

Figure 5 shows *different* results for $|\Phi_{\text{GHZ}}\rangle$ and $|\Phi_{\text{BP}}\rangle$, which is mainly due to the one biseparability of $|\Phi_{\text{BP}}\rangle$, making the FDM ent the only measure of these three that distinguishes between the separability of these states, and yet does not neglect the other bipartite entanglement correlations in $|\Phi_{\text{BP}}\rangle$. Again, $|\Phi_{\text{F}}\rangle$ seems to outperform all other states in every measure, as suggested by the fact that $|\psi_{\text{Rand}}\rangle$ seems to approach its performance, and $|\psi_{\text{W}}\rangle$ slightly underperforms in every area.

D. Comparison of FGM, FSM, and FDM Ents

The most important difference between Υ_{FGM} and both Υ_{FSM} and Υ_{FDM} is that $\Upsilon_{\text{GM}_2}(\rho_{|\Phi_{\text{BP}}\rangle}) = 0$ while $\tilde{\Upsilon}_{\text{SM}_2}(\rho_{|\Phi_{\text{BP}}\rangle}) \neq 0$ and $\tilde{\Upsilon}_{\text{DM}_2}(\rho_{|\Phi_{\text{BP}}\rangle}) \neq 0$. The fact that not all bipartitions of $|\Phi_{\text{BP}}\rangle$ are separable means that there are *some* bipartitions that have *entanglement correlations*, and the *sum* over all 2-partitional quantities in $\tilde{\Upsilon}_{\text{SM}_2}$ and $\tilde{\Upsilon}_{\text{DM}_2}$ is why they detect these correlations, while the *minimum* over all 2-partitions in Υ_{GM_2} is why it *misses those entanglement correlations*, reporting “zero.” Therefore Υ_{GM_2} is *not sufficient to detect all entanglement correlations of 2-partitions of a state*, so Υ_{FGM} is not sufficient to detect all entanglement correlations.

Thus, we must make an important new distinction; *presence of separability in a particular k -partition is not sufficient to claim absence of entanglement correlations over all k -partitions for a given k* . Since *nonseparable nonlocal correlations* (NSNLC) are what the word *entanglement* really means, we must require *the necessary and sufficient detection of the presence of any NSNLC* as our prime criterion for what constitutes an entanglement measure. We state all of this in the following theorem.

True-Entanglement Theorem: The *absence of separability between any partitions* is necessary and sufficient for the *presence of any entanglement correlations*, and

therefore the presence of true entanglement. In other words; the *presence of separability between all partitions* is necessary and sufficient for the *absence of all entanglement correlations*, and thus the absence of true entanglement.

This theorem reflects the fact that although a state may be separable over one particular k -partition, that is not sufficient to conclude the absence of all k -partite entanglement correlations, so sub- N k -separability is not a sufficient criterion for the absence of all k -partite NSNLC.

The likely reason that GM_k -entanglement was defined with the min function is that the presence of separability in any one bipartition *is* sufficient to claim the absence of entanglement correlations for *bipartite* systems, since there is *only one bipartition*. So if separability were our only concern for multimode systems, then GM_k -entanglement would be correctly defined because if a state is in *any way k -separable*, then its GM_k -entanglement is 0. (After all, GM measures *do* correctly indicate whether a pure state is a product over at least one k -partition.) But since we have just seen examples that k -separability is not sufficient to conclude the absence of all k -partite NSNLC, and since NSNLC are what entanglement *really is*, then GM_k -“entanglement” is *not* really a measure of k -partite entanglement.

Unfortunately, there is now quite a lot of literature that uses the terminology (GM)-“ k -entangled” to describe a condition that is insufficient to determine the presence of entanglement correlations over all k -partitions. Our remedy for this was to observe the fact that the absence of k -separability is the condition of all k -partitions not having k -mode product form, which motivated us to sum the N -mode k -partitional entanglement values over all k -partitions in our various candidate entanglement measures in Sec. II. These sums gave us candidate F_k -entanglement values which were further added over all k values to construct candidate measures for detecting all possible entanglement correlations in a given pure state.

However, the True-Entanglement Theorem alone is not sufficient to *distinguish between* states like $|\Phi_{\text{GHZ}}\rangle$ and $|\Phi_{\text{BP}}\rangle$. One missing concept is that the states that are most entangled have the most *simultaneous* entanglement correlations over all possible partitions. Since this is exactly what the FSM ent measures, then it is both necessary and sufficient to *detect* all entanglement correlations, *and* it measures their simultaneous presence, providing an *ordering* for multipartite entangled states.

Yet the FSM ent’s ordering is *still* not sufficient to reveal the difference between states like $|\Phi_{\text{GHZ}}\rangle$ and $|\Phi_{\text{BP}}\rangle$, as seen in Fig. 4. Therefore, by also requiring that the simultaneous entanglement correlations be *as evenly and as widely distributed as possible*, we attain ordering criteria that distinguish $|\Phi_{\text{GHZ}}\rangle$ and $|\Phi_{\text{BP}}\rangle$ without sacrificing information about entanglement correlations. The FDM ent (ent-concurrence) may achieve this, as seen in Fig. 5.

However, the True-Entanglement Theorem *only applies to applications of entanglement in the full Hilbert space of ρ* . For applications of entanglement in the *reductions*, other principles are involved, as discussed in Sec. VII.

IV. CANDIDATE MIXED-STATE MEASURES

Here we list the mixed-state entanglement-measure candidates that we test in Sec. V. In all cases, $\hat{E}(\rho)$ means the convex-roof extension of a pure-state measure $E(\rho)$ to handle mixed-state input (see [21, App. J]).

1. The FGM ent of formation (using $\Upsilon_{\text{FGM}}(\rho)$ from (6)):

$$\hat{\Upsilon}_{\text{FGM}}(\rho) \equiv \min_{\{p_j, \rho_j\} | \rho = \sum_j p_j \rho_j} \left(\sum_j p_j \Upsilon_{\text{FGM}}(\rho_j) \right). \quad (16)$$

2. The strict FGM (SFGM) ent of formation:

$$\Upsilon_{\text{SFGM}}(\rho) \equiv \frac{1}{M_{\text{SFGM}}} \sum_{k=2}^N \Upsilon_{\text{SGM}_k}(\rho), \quad (17)$$

where M_{SFGM} is a normalization factor, and the strict GM_k (SGM_k) ent of formation is

$$\Upsilon_{\text{SGM}_k}(\rho) \equiv \min(\{\hat{\Upsilon}^{(\mathbf{N}_k^{(k)})}(\rho)\}), \quad (18)$$

where $\{\hat{\Upsilon}^{(\mathbf{N}_k^{(k)})}(\rho)\}$ is the set of *convex-roof extensions* of all N -mode k -partitional ents. Here, the minimum *over all convex-roof-extensions* of a given kind of k -partitional ent ensures that if a state achieves *strict k -separability*, *all* of its optimal-decomposition pure states are *k -separable over the same partitions*.

3. The FSM ent of formation (using $\Upsilon_{\text{FSM}}(\rho)$ from (8)):

$$\hat{\Upsilon}_{\text{FSM}}(\rho) \equiv \min_{\{p_j, \rho_j\} | \rho = \sum_j p_j \rho_j} \left(\sum_j p_j \Upsilon_{\text{FSM}}(\rho_j) \right). \quad (19)$$

4. The FDM ent of formation (with $\Upsilon_{\text{FDM}}(\rho)$ from (10)):

$$\hat{\Upsilon}_{\text{FDM}}(\rho) \equiv \min_{\{p_j, \rho_j\} | \rho = \sum_j p_j \rho_j} \left(\sum_j p_j \Upsilon_{\text{FDM}}(\rho_j) \right). \quad (20)$$

We do not use a “hat” if a convex-roof extension (CRE) has been applied already within the function.

V. TESTS OF CANDIDATE MIXED-STATE MEASURES

Limiting ourselves to rank-2 mixed states (since CREs of those are practical to approximate) we use test states,

$$\begin{aligned} \rho_{\text{GHZ}+1} &\equiv \frac{1}{2}(|\Phi_{\text{GHZ}}\rangle\langle\Phi_{\text{GHZ}}| + |1,1,1,1\rangle\langle 1,1,1,1|) \\ \rho_{2\text{-sep}} &\equiv \frac{1}{2}(\rho_{|\Phi^+\rangle} \otimes |\Phi^+\rangle + \rho_{|1\rangle}^{(1)} \otimes |\Phi_{\text{GHZ}_3}\rangle\langle\Phi_{\text{GHZ}_3}|) \\ \rho_{\text{F}+1} &\equiv \frac{1}{2}(|\Phi_{\text{F}}\rangle\langle\Phi_{\text{F}}| + |1,1,1,1\rangle\langle 1,1,1,1|) \\ \rho_{\text{MME}} &\equiv \frac{1}{2}(\rho_{\frac{1}{\sqrt{2}}(|1,1,1,1\rangle + |2,2,2,1\rangle)} + \rho_{\frac{1}{\sqrt{2}}(|1,1,1,2\rangle + |2,2,2,2\rangle)}) \\ \rho_{|\Phi_{\text{F}}\rangle} &\equiv |\Phi_{\text{F}}\rangle\langle\Phi_{\text{F}}|, \end{aligned} \quad (21)$$

where $\rho_{|A\rangle} \equiv |A\rangle\langle A|$, and $|\Phi_{\text{GHZ}}\rangle$, $|\Phi^+\rangle \otimes |\Phi^+\rangle \equiv |\Phi_{\text{BP}}\rangle$, and $|\Phi_{\text{F}}\rangle$ are from (14), $\rho_{|1\rangle}^{(1)}$ is the first computational basis state for the mode-1 qubit, and $|\Phi_{\text{GHZ}_3}\rangle \equiv \frac{1}{\sqrt{2}}(|1,1,1\rangle\langle 1,1,1| + |2,2,2\rangle\langle 2,2,2|)$ is a 3-qubit GHZ state.

We include $\rho_{\text{GHZ}+1}$ and $\rho_{\text{F}+1}$ because they are mixtures of highly entanglement-correlated states with a basis state they already include, to see how the candidate measures rate this lowering of entanglement correlation.

To test a state like (2), $\rho_{2\text{-sep}}$ decomposes into pure states that are each 2-separable *in different ways*, where each part has strong internal entanglement correlations.

The state ρ_{MME} , when viewed as a 2×8 system is a *mixed state with the same entanglement as a maximally entangled pure state*. Rediscovered in the present work, this phenomenon was originally discovered in [26, 27], and called “mixed maximally entangled (MME) states.” It is easy to prove that *all* decompositions of such states consist of maximally entangled pure decomposition states, yielding an entanglement of 1 by any unit-normalized convex-roof (or nearest-separable-state [28]) measure.

We use *pure state* $\rho_{|\Phi_{\text{F}}\rangle}$ as a reference since it had near-highest values in the GM measures of Fig. 3, and it may have the highest values for the SM measures in Fig. 4 and the DM measures in Fig. 5.

A. Tests and Analysis of Mixed-Input FGM Ents

Figures 6–7 show similar results but differ in subtle ways briefly explained after each.

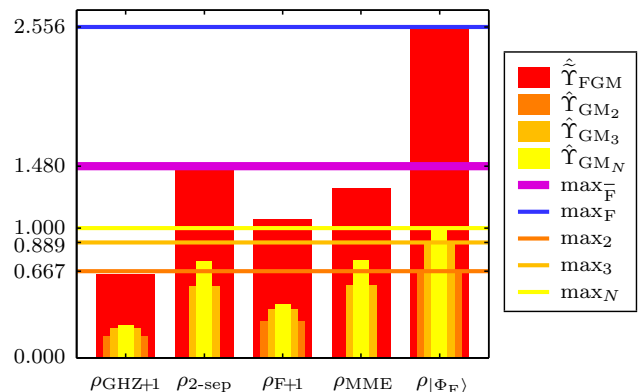


FIG. 6: (color online) Unnormalized FGM ent of formation $\hat{\Upsilon}_{\text{FGM}}$ of (16) approximated for the test states of (21). The (normalized) GM_k ents of formation $\hat{\Upsilon}_{\text{GM}_k}$ (CREs of (7)) are also approximated, and the maximum of each over all test states is $\text{max}_k \equiv \max(\hat{\Upsilon}_{\text{GM}_k})$, while $\text{max}_{\bar{\text{F}}} \equiv \max(\hat{\Upsilon}_{\text{FGM}})$ applies to all non- $\rho_{|\Phi_{\text{F}}\rangle}$ test states, and $\text{max}_{\text{F}} \equiv \max(\hat{\Upsilon}_{\text{FGM}}(\rho_{|\Phi_{\text{F}}\rangle}))$. The CRE approximations used 900 decompositions, as in [21].

The main items of interest in Fig. 6 are the fact that both $\rho_{2\text{-sep}}$ and ρ_{MME} have $\hat{\Upsilon}_{\text{GM}_2} = 0$, and while we expect this to be true from the way the FGM ent minimizes over all bipartitions for each decomposition state within the larger minimization of the CRE, it shows that GM measures *ignore* entanglement correlations, since ρ_{MME} in particular has the maximal entanglement of a pure state for the $(1|2, 3, 4)$ bipartition, as mentioned earlier.

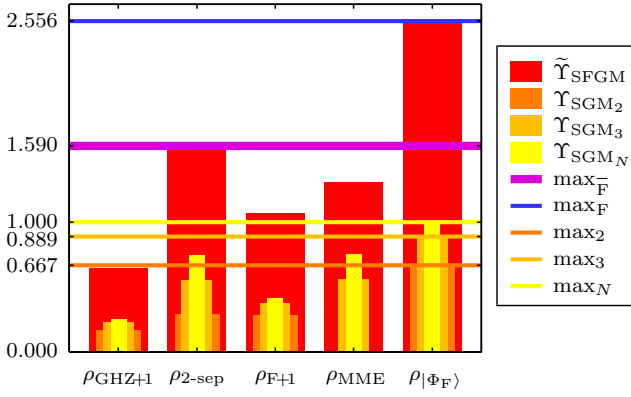


FIG. 7: (color online) Unnormalized SFGM ent of formation \tilde{Y}_{SFGM} of (17) approximated for the test states of (21). The (normalized) SGM $_k$ ents of formation Υ_{SGM_k} of (18) are also approximated, and the maximum of each over all test states is $\max_k \equiv \max(\Upsilon_{\text{SGM}_k})$, while $\max_{\bar{F}} \equiv \max(\tilde{Y}_{\text{SFGM}})$ applies to all non $\rho_{|\Phi_F\rangle}$ test states, and $\max_F \equiv \max(\tilde{Y}_{\text{SFGM}}(\rho_{|\Phi_F\rangle}))$. CRE approximations used 900 decompositions.

The *strict* version, the SFGM ent of formation \tilde{Y}_{SFGM} in Fig. 7 does slightly better than \hat{Y}_{FGM} in Fig. 6 because it correctly detects that no bipartitions of $\rho_{2\text{-sep}}$ are without entanglement correlation since its $\Upsilon_{\text{SGM}_2} \neq 0$, but it still *completely ignores* the maximal bipartite entanglement correlation in ρ_{MME} , for which $\Upsilon_{\text{SGM}_2} = 0$.

We discuss further issues with GM measures regarding states like $\rho_{2\text{-sep}}$ and (2) in App. H.

B. Tests and Analysis of Mixed-Input FSM Ent

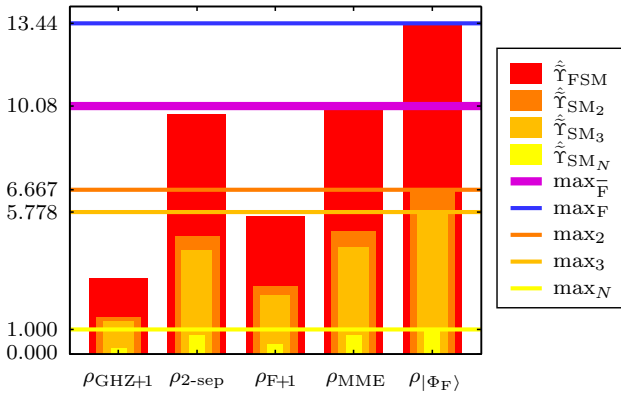


FIG. 8: (color online) Unnormalized FSM ent of formation \tilde{Y}_{FSM} of (19) approximated for the test states of (21). The unnormalized SM $_k$ ents of formation \tilde{Y}_{SM_k} (CREs of (9)) are also approximated, and the maximum of each over all test states is $\max_k \equiv \max(\tilde{Y}_{\text{SM}_k})$, while $\max_{\bar{F}} \equiv \max(\tilde{Y}_{\text{FSM}})$ applies to all non $\rho_{|\Phi_F\rangle}$ test states, and $\max_F \equiv \max(\tilde{Y}_{\text{FSM}}(\rho_{|\Phi_F\rangle}))$. CRE approximations used 900 decompositions.

Figure 8 tests unnormalized FSM ent of formation from (19), and we see that the known bipartite entanglement

correlations in both $\rho_{2\text{-sep}}$ and ρ_{MME} are detected since $\hat{Y}_{\text{SM}_2} \neq 0$ for each.

C. Tests and Analysis of Mixed-Input FDM Ent (The Ent-Concurrence)

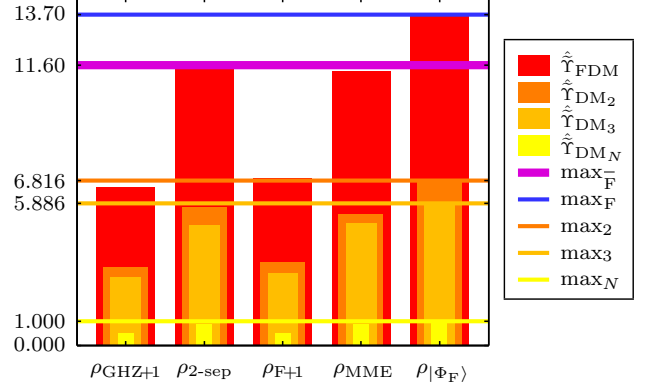


FIG. 9: (color online) Unnormalized FDM ent of formation (ent-concurrence of formation) \hat{Y}_{FDM} of (20) approximated for the test states of (21). The unnormalized DM $_k$ ents of formation \hat{Y}_{DM_k} (CREs of (11)) are also approximated, and the maximum of each over all test states is $\max_k \equiv \max(\hat{Y}_{\text{DM}_k})$, while $\max_{\bar{F}} \equiv \max(\hat{Y}_{\text{FDM}})$ applies to all non $\rho_{|\Phi_F\rangle}$ test states, and $\max_F \equiv \max(\hat{Y}_{\text{FDM}}(\rho_{|\Phi_F\rangle}))$. CRE approximations used 900 decompositions.

Here in Fig. 9, we see the ratings of \hat{Y}_{FDM} are similar to those of \hat{Y}_{FSM} in Fig. 8, except that here, the values for $\rho_{\text{GHZ}+1}$ are much closer to the values for $\rho_{\text{F}+1}$ (though still less than they are). Thus, this test does not show any apparent problems, and exhibits the necessary features that neither $\rho_{2\text{-sep}}$ nor ρ_{MME} can be considered free of 2-partite entanglement correlations (see App. H).

D. Comparison of all Mixed-Input Candidates

The main difference between the GM measures (from (16) and (17)) and the SM and DM measures of (19) and (20) is that the GM measures tend to undervalue the amount of entanglement, which is a consequence of their interpretation of separability as the prime criterion for lack of entanglement. The SM and DM measures take a more global approach, checking every possible k -partition for the presence of entanglement correlations, and as such, they correctly detect entanglement of every k -partitional type, in particular correctly not ignoring the maximal bipartite entanglement in ρ_{MME} .

In the pure-input case, the FDM ent Υ_{FDM} was the only measure that could distinguish between $|\Phi_{\text{GHZ}}\rangle$ and $|\Phi_{\text{BP}}\rangle$ *without* sacrificing detection of entanglement correlations, *and* it equals the concurrence C for two qubits. Since C for *mixed* states is a convex-roof extension (CRE), and since \hat{Y}_{FDM} is *also* a CRE, then $\hat{Y}_{\text{FDM}} = C$ for *mixed two-qubit states*, as well.

VI. ENT-CONCURRENCE

The ability of $\hat{\Upsilon}_{\text{FDM}}$ to detect and distinguish multipartite entanglement correlations and its link to C both suggest that we adopt it as a universal measure of multipartite entanglement, called the *ent-concurrence*,

$$\hat{C}_{\Upsilon}(\rho) \equiv \hat{\Upsilon}_{\text{FDM}}(\rho), \quad (22)$$

where $\hat{\Upsilon}_{\text{FDM}}$ is defined in (20), so that

$$\hat{C}_{\Upsilon}(\rho) \equiv \min_{\{p_j, \rho_j\} | \rho = \sum_j p_j \rho_j} \left(\sum_j p_j \sum_{k=2}^N \frac{1}{M_k} \sum_{h=1}^{\{N\}_k} \sqrt{\Upsilon^{(\mathbf{N}_h^{(k)})}(\rho_j)} \right), \quad (23)$$

where $M_k \equiv M_{\text{FDM}} M_{\text{DM}_k}$ is a normalization factor based on those of (10) and (11), and $\{N\}_k$ are Stirling numbers of the second kind as in (9), which is the number of different N -mode k -partitional ents $\Upsilon^{(\mathbf{N}_h^{(k)})}(\rho)$.

While \hat{C}_{Υ} detects all entanglement and distinguishes between different types of F_k -entanglement, it may also be useful to have a partition-specific view of how much entanglement exists between particular mode groups. Therefore, in the notation of [21], we also define the *N -mode partitional ent-concurrence vector* as

$$\Xi_{C_{\Upsilon}}^{(\mathbf{N})}(\rho) \equiv \begin{pmatrix} \{\hat{C}_{\Upsilon}^{(\mathbf{N}_h^{(2)})}(\rho)\} \\ \vdots \\ \{\hat{C}_{\Upsilon}^{(\mathbf{N}_h^{(N)})}(\rho)\} \end{pmatrix}, \quad (24)$$

where $\{\hat{C}_{\Upsilon}^{(\mathbf{N}_h^{(k)})}(\rho)\}$ is the set of all N -mode k -partitional ent-concurrences of formation, the pure-input versions of which are in (13). For example, in a 4-mode system,

$$\Xi_{C_{\Upsilon}}^{(4)} \equiv \Xi_{C_{\Upsilon}}^{(1,2,3,4)} = \begin{pmatrix} \hat{C}_{\Upsilon}^{(1|234)} \hat{C}_{\Upsilon}^{(2|134)} \hat{C}_{\Upsilon}^{(3|124)} \hat{C}_{\Upsilon}^{(4|123)} \hat{C}_{\Upsilon}^{(1,2|34)} \hat{C}_{\Upsilon}^{(1,3|24)} \hat{C}_{\Upsilon}^{(1,4|23)} \\ \hat{C}_{\Upsilon}^{(1|2|34)} \hat{C}_{\Upsilon}^{(1|3|24)} \hat{C}_{\Upsilon}^{(1|4|23)} \hat{C}_{\Upsilon}^{(2|3|14)} \hat{C}_{\Upsilon}^{(2|4|13)} \hat{C}_{\Upsilon}^{(3|4|12)} \\ \hat{C}_{\Upsilon}^{(1|2|3|4)} \end{pmatrix}, \quad (25)$$

where, for instance,

$$\hat{C}_{\Upsilon}^{(2|1,3,4)} = \min_{\{p_j, \rho_j\} | \rho = \sum_j p_j \rho_j} \left(\sum_j p_j \sqrt{\Upsilon^{(2|1,3,4)}(\rho_j)} \right). \quad (26)$$

Thus, the top row of $\Xi_{C_{\Upsilon}}^{(\mathbf{N})}$ lists all contributions to F_2 -entanglement, and so-on until the lowest row gives the F_N -entanglement, yielding a fine-grained view of the entanglement between each possible mode group.

For an intermediate view of entanglement, we can define the *N -mode k -ent-concurrences of formation* as

$$\hat{C}_{\Upsilon_k}(\rho) \equiv \hat{\Upsilon}_{\text{DM}_k}(\rho), \quad (27)$$

which is a CRE of a 1-norm over all $C_{\Upsilon}^{(\mathbf{N}_h^{(k)})}(\rho)$ for a given k , as seen from (13) and the definition of $\Upsilon_{\text{DM}_k}(\rho)$ in (11).

Hierarchy of Maximally F_N -Entangled TGX States

The ent-concurrence identifies a hierarchy among the maximally F_N -entangled states, which is easiest to see by examining its values for the subset of F_N -entangled TGX states from App. G, as in Table I.

TABLE I: Normalized ent-concurrence C_{Υ} and normalized k -ent-concurrences C_{Υ_k} for each of the maximally F_N -entangled 4-qubit TGX states $|\Phi_j^{[L_*]}\rangle$ involving the first computational basis state $|1\rangle \equiv |1,1,1,1\rangle$, from App. G, where L_* is the number of levels with nonzero state coefficients. Normalizations are over these states alone, and may not be the normalizations over all states. The test states of (14) are $|\Phi_{\text{GHZ}}\rangle \equiv |\Phi_1^{[2]}\rangle$, $|\Phi_{\text{BP}}\rangle \equiv |\Phi_1^{[4]}\rangle$, and $|\Phi_{\text{F}}\rangle \equiv |\Phi_2^{[4]}\rangle$, in the first three rows.

$ \Phi_j^{[L_*]}\rangle$	C_{Υ}	C_{Υ_2}	C_{Υ_3}	C_{Υ_N}
$ \Phi_1^{[2]}\rangle$	0.957	0.946	0.961	1.000
$ \Phi_1^{[4]}\rangle$	0.922	0.880	0.957	1.000
$ \Phi_2^{[4]}\rangle$	1.000	1.000	1.000	1.000
$ \Phi_3^{[4]}\rangle$	0.922	0.880	0.957	1.000
$ \Phi_4^{[4]}\rangle$	1.000	1.000	1.000	1.000
$ \Phi_5^{[4]}\rangle$	0.922	0.880	0.957	1.000
$ \Phi_6^{[4]}\rangle$	1.000	1.000	1.000	1.000
$ \Phi_7^{[4]}\rangle$	1.000	1.000	1.000	1.000
$ \Phi_8^{[4]}\rangle$	1.000	1.000	1.000	1.000
$ \Phi_9^{[4]}\rangle$	1.000	1.000	1.000	1.000
$ \Phi_1^{[6]}\rangle$	0.957	0.946	0.961	1.000
$ \Phi_2^{[6]}\rangle$	0.957	0.946	0.961	1.000
$ \Phi_3^{[6]}\rangle$	0.957	0.946	0.961	1.000
$ \Phi_1^{[8]}\rangle$	0.957	0.946	0.961	1.000

In Table I, the highest-rated maximally F_N -entangled TGX states, having $(C_{\Upsilon}, C_{\Upsilon_2}, C_{\Upsilon_3}, C_{\Upsilon_N}) = (1, 1, 1, 1)$, are the *tier-1 F_N -entangled states*,

$$\begin{aligned} |\Phi_2^{[4]}\rangle &= \frac{1}{\sqrt{4}}(|1111\rangle + |1122\rangle + |2212\rangle + |2221\rangle) \\ |\Phi_4^{[4]}\rangle &= \frac{1}{\sqrt{4}}(|1111\rangle + |1212\rangle + |2122\rangle + |2221\rangle) \\ |\Phi_6^{[4]}\rangle &= \frac{1}{\sqrt{4}}(|1111\rangle + |1221\rangle + |2122\rangle + |2212\rangle) \\ |\Phi_7^{[4]}\rangle &= \frac{1}{\sqrt{4}}(|1111\rangle + |1222\rangle + |2112\rangle + |2221\rangle) \\ |\Phi_8^{[4]}\rangle &= \frac{1}{\sqrt{4}}(|1111\rangle + |1222\rangle + |2121\rangle + |2212\rangle) \\ |\Phi_9^{[4]}\rangle &= \frac{1}{\sqrt{4}}(|1111\rangle + |1222\rangle + |2122\rangle + |2211\rangle), \end{aligned} \quad (28)$$

where $|abcd\rangle \equiv |a,b,c,d\rangle$. The *tier-2 F_N -entangled states*,

with $(C_{\mathcal{R}}, C_{\mathcal{R}_2}, C_{\mathcal{R}_3}, C_{\mathcal{R}_N}) \approx (0.957, 0.946, 0.961, 1)$, are

$$\begin{aligned} |\Phi_1^{[2]}\rangle &= \frac{1}{\sqrt{2}}(|1111\rangle + |2222\rangle) \\ |\Phi_1^{[6]}\rangle &= \frac{1}{\sqrt{6}}(|1111\rangle + |1122\rangle + |1212\rangle + |2121\rangle + |2211\rangle + |2222\rangle) \\ |\Phi_2^{[6]}\rangle &= \frac{1}{\sqrt{6}}(|1111\rangle + |1122\rangle + |1221\rangle + |2112\rangle + |2211\rangle + |2222\rangle) \\ |\Phi_3^{[6]}\rangle &= \frac{1}{\sqrt{6}}(|1111\rangle + |1212\rangle + |1221\rangle + |2112\rangle + |2121\rangle + |2222\rangle) \\ |\Phi_1^{[8]}\rangle &= \frac{1}{\sqrt{8}}(|1111\rangle + |1122\rangle + |1212\rangle + |1221\rangle \\ &\quad + |2112\rangle + |2121\rangle + |2211\rangle + |2222\rangle), \end{aligned} \quad (29)$$

and the lowest-rated group, the *tier-3* F_N -entangled states, with $(C_{\mathcal{R}}, C_{\mathcal{R}_2}, C_{\mathcal{R}_3}, C_{\mathcal{R}_N}) \approx (0.922, 0.880, 0.957, 1)$, are

$$\begin{aligned} |\Phi_1^{[4]}\rangle &= \frac{1}{\sqrt{4}}(|1111\rangle + |1122\rangle + |2211\rangle + |2222\rangle) \\ |\Phi_3^{[4]}\rangle &= \frac{1}{\sqrt{4}}(|1111\rangle + |1212\rangle + |2121\rangle + |2222\rangle) \\ |\Phi_5^{[4]}\rangle &= \frac{1}{\sqrt{4}}(|1111\rangle + |1221\rangle + |2112\rangle + |2222\rangle). \end{aligned} \quad (30)$$

All of these states are maximally F_N -entangled, as seen in Table I, and furthermore, these are only a small portion of the “phaseless” maximally F_N -entangled TGX states, since similar sets can be generated by specifying a different common “starting level” than $|1\rangle = |1111\rangle$.

Whether or not other states exist that have higher ent-concurrence than the tier-1 states is still unknown, but none were found in the present numerical tests.

To see the most fine-grained view, from (25) the N -mode ent-concurrence vectors of $|\Phi_F\rangle \equiv |\Phi_2^{[4]}\rangle$ (tier 1), $|\Phi_{\text{GHZ}}\rangle \equiv |\Phi_1^{[2]}\rangle$ (tier 2), and $|\Phi_{\text{BP}}\rangle \equiv |\Phi_1^{[4]}\rangle$ (tier 3) are

$$\Xi_{C_{\mathcal{R}}}^{(N)}(\rho_{|\Phi_F\rangle}) = \begin{pmatrix} 1 & 1 & 1 & 1 & \sqrt{\frac{2}{3}} & 1 & 1 \\ \sqrt{\frac{8}{9}} & 1 & 1 & 1 & 1 & \sqrt{\frac{8}{9}} & \\ & & & & & & 1 \end{pmatrix}, \quad (31)$$

$$\Xi_{C_{\mathcal{R}}}^{(N)}(\rho_{|\Phi_{\text{GHZ}}\rangle}) = \begin{pmatrix} 1 & 1 & 1 & 1 & \sqrt{\frac{2}{3}} & \sqrt{\frac{2}{3}} & \sqrt{\frac{2}{3}} \\ \sqrt{\frac{8}{9}} & \sqrt{\frac{8}{9}} & \sqrt{\frac{8}{9}} & \sqrt{\frac{8}{9}} & \sqrt{\frac{8}{9}} & \sqrt{\frac{8}{9}} & \sqrt{\frac{8}{9}} \\ & & & & & & 1 \end{pmatrix}, \quad (32)$$

$$\Xi_{C_{\mathcal{R}}}^{(N)}(\rho_{|\Phi_{\text{BP}}\rangle}) = \begin{pmatrix} 1 & 1 & 1 & 1 & 0 & 1 & 1 \\ \sqrt{\frac{2}{3}} & 1 & 1 & 1 & 1 & \sqrt{\frac{2}{3}} & \\ & & & & & & 1 \end{pmatrix}. \quad (33)$$

The sum of all elements in each of (31–33) is the unnormalized ent-concurrence, yielding 13.70, 13.11, and 12.63, respectively, which are the first three Υ_{FDM} values (in a different order) in Fig. 5. In contrast, the square of all the elements in (31–33) (since these are pure states), yields the N -mode ent vectors of [21], the sums of which yield 13.44, 12.33, and 12.33, respectively, which explains why the values of Υ_{FSM} for $|\Phi_{\text{GHZ}}\rangle$ and $|\Phi_{\text{BP}}\rangle$ are equal in Fig. 4, showing that the FSM measures were not able to distinguish these two states.

The worth of $\Xi_{C_{\mathcal{R}}}^{(N)}$ is that it shows us *between which mode groups* entanglement and separability occur. For

example, the 0 in (33) shows that the mode groups defined by the partitioning (1,2|3,4) are separable in $\rho_{|\Phi_{\text{BP}}\rangle}$, which is true since that is the Bell product, but (33) *also* shows that the *entanglement is maximal* between all other bipartitions of the state (seen in its top row). Thus, the ent-concurrence does not ignore all of these bipartite entanglement correlations just because one of them is zero, as the GM measures do.

VII. ABSOLUTE ENT-CONCURRENCE

While the ent-concurrence (and its accompanying notions of N -mode partitional ent-concurrence vector and k -ent-concurrence) evaluates the multipartite entanglement resources of *the entire input state in its full space*, another dimension of details can be gleaned by evaluating the entanglement *within reductions of the input state*.

Thus for mode group \mathbf{m} , the S -mode partitional ent-concurrence vector is

$$\Xi_{C_{\mathcal{R}}}^{(\mathbf{m})}(\rho) \equiv \begin{pmatrix} \{\hat{C}_{\mathcal{R}}^{(\mathbf{m}_h^{(2)})}(\rho)\} \\ \vdots \\ \{\hat{C}_{\mathcal{R}}^{(\mathbf{m}_h^{(S)})}(\rho)\} \end{pmatrix}, \quad (34)$$

where $\mathbf{m} \equiv (m_1, \dots, m_S)$; $S \in 2, \dots, N$ are the modes to which $\rho \equiv \rho^{(1, \dots, N)}$ is being reduced before being partitioned, and $\{\hat{C}_{\mathcal{R}}^{(\mathbf{m}_h^{(T)})}\}$ is the set of all S -mode T -partitional ent-concurrences of a given reduction $\check{\rho}^{(\mathbf{m})}$ where $T \in 2, \dots, S$, where for a particular partitioning labeled by h , the *partitional ent-concurrence* is

$$\hat{C}_{\mathcal{R}}^{(\mathbf{m}_h^{(T)})}(\rho) \equiv \min_{\{p_j, \rho_j\}_{\rho = \sum_j p_j \rho_j}} \left(\sum_j p_j \sqrt{\Upsilon^{(\mathbf{m}_h^{(T)})}(\rho_j)} \right), \quad (35)$$

where $\Upsilon^{(\mathbf{m}_h^{(T)})}$ is the *partitional ent* (of h -labeled partition $\mathbf{m}_h^{(T)}$) mentioned after (5) and defined in detail in [21]. Thus, row $T-1$ of $\Xi_{C_{\mathcal{R}}}^{(\mathbf{m})}$ lists all possible T -partitional ent-concurrences of the mode- \mathbf{m} reduction of ρ .

Since a partitional ent-concurrence vector exists for each reduction \mathbf{m} , we can define the *ent-concurrence array* as the matrix $\tilde{\nabla}_{C_{\mathcal{R}}}$ (not a gradient) whose elements are partitional ent-concurrence vectors,

$$(\tilde{\nabla}_{C_{\mathcal{R}}})_{k,l}(\rho) \equiv \Xi_{C_{\mathcal{R}}}^{((\text{nCk}(\mathbf{c},k))_{l,\dots})}, \quad (36)$$

where $\mathbf{c} \equiv (1, \dots, N)$, $k \in 2, \dots, N$, and $l \in 1, \dots, \binom{N}{k}$ where $\binom{N}{k} \equiv \frac{N!}{k!(N-k)!}$, and $\text{nCk}(\mathbf{v}, k)$ is the vectorized n -choose- k function yielding the matrix whose rows are each unique combinations of the elements of \mathbf{v} chosen k at a time, and $A_{l,\dots}$ is the l th row of matrix A . For example in $N = 4$, (suppressing input arguments ρ)

$$\tilde{\nabla}_{C_{\mathcal{R}}}(\rho) = \begin{pmatrix} \Xi_{C_{\mathcal{R}}}^{(1,2)} & \Xi_{C_{\mathcal{R}}}^{(1,3)} & \Xi_{C_{\mathcal{R}}}^{(1,4)} & \Xi_{C_{\mathcal{R}}}^{(2,3)} & \Xi_{C_{\mathcal{R}}}^{(2,4)} & \Xi_{C_{\mathcal{R}}}^{(3,4)} \\ & \Xi_{C_{\mathcal{R}}}^{(1,2,3)} & \Xi_{C_{\mathcal{R}}}^{(1,2,4)} & \Xi_{C_{\mathcal{R}}}^{(1,3,4)} & \Xi_{C_{\mathcal{R}}}^{(2,3,4)} & \\ & & & \Xi_{C_{\mathcal{R}}}^{(1,2,3,4)} & & \end{pmatrix}, \quad (37)$$

where the 2-mode partitional ent-concurrence vectors have just one element, such as

$$\Xi_{C_{\mathcal{R}}}^{(2,3)} = \hat{C}_{\mathcal{R}}^{(2|3)} = \hat{C}_{\mathcal{R}}^{(2,3)}, \quad (38)$$

and 3-mode partitional ent-concurrence vectors look like

$$\Xi_{C_{\mathcal{R}}}^{(1,2,4)} = \begin{pmatrix} \hat{C}_{\mathcal{R}}^{(1|2,4)} & \hat{C}_{\mathcal{R}}^{(2|1,4)} & \hat{C}_{\mathcal{R}}^{(4|1,2)} \\ \hat{C}_{\mathcal{R}}^{(1|2,4)} & \hat{C}_{\mathcal{R}}^{(1|2|4)} & \\ \hat{C}_{\mathcal{R}}^{(2|1,4)} & & \end{pmatrix}, \quad (39)$$

and the 4-mode partitional ent-concurrence vector $\Xi_{C_{\mathcal{R}}}^{(1,2,3,4)}$ is given by (25).

Then, to create a universal multipartite entanglement measure that can detect *all possible* entanglement correlations of a state *including those of all of its reductions*, we can define the *absolute ent-concurrence* as

$$C_{\mathcal{R}_{\text{abs}}}(\rho) \equiv \frac{\|\tilde{\nabla}_{C_{\mathcal{R}}}(\rho)\|_1}{\max(\|\tilde{\nabla}_{C_{\mathcal{R}}}(\rho)\|_1)}, \quad (40)$$

which is the 1-norm over all partitional ent-concurrences normalized to its maximum value over all input states.

Thus, by Theorem 1 from App. D, $C_{\mathcal{R}_{\text{abs}}}$ captures a measurement of all possible ways in which a state can be entanglement-correlated. The main drawback of the absolute ent-concurrence of (40) is that it generally requires convex-roof extensions (CREs) in all elements of $\tilde{\nabla}_{C_{\mathcal{R}}}$, *even when the input is pure*, since *reductions* of the pure decomposition states ρ_j of ρ are generally mixed. This means that it is usually computationally intractable to calculate $C_{\mathcal{R}_{\text{abs}}}$, even for pure ρ .

For states like $|\psi_{\mathcal{W}}\rangle$, where one of its prime characteristics is that it retains entanglement after the removal of a particle (tracing away a mode) [24], finding the entanglement of its *reductions* is possible with the absolute ent-concurrence, and the ent-concurrence array of (36) is an excellent tool for a high-resolution picture of all possible entanglement correlations of the state. These measures would certainly show exactly how $|\psi_{\mathcal{W}}\rangle$ differs from $|\Phi_{\text{GHZ}}\rangle$, which is separable after removal of any particles. For example, the ent-concurrence array of $|\psi_{\mathcal{W}}\rangle$ is

$$\tilde{\nabla}_{C_{\mathcal{R}}}(\rho_{|\psi_{\mathcal{W}}\rangle}) = \begin{pmatrix} \left(\begin{array}{cccccc} \frac{1}{2} & \frac{1}{2} & \frac{1}{2} & \frac{1}{2} & \frac{1}{2} & \frac{1}{2} \\ \left(\sqrt{\frac{1}{2}} \sqrt{\frac{1}{2}} \sqrt{\frac{1}{2}} \right) & \left(\sqrt{\frac{1}{2}} \sqrt{\frac{1}{2}} \sqrt{\frac{1}{2}} \right) \\ \sqrt{\frac{1}{2}} & \sqrt{\frac{1}{2}} & \sqrt{\frac{1}{2}} & \sqrt{\frac{1}{2}} & \sqrt{\frac{1}{2}} & \sqrt{\frac{1}{2}} \end{array} \right) \\ \left(\begin{array}{cccccc} \sqrt{\frac{3}{4}} & \sqrt{\frac{3}{4}} & \sqrt{\frac{3}{4}} & \sqrt{\frac{3}{4}} & \sqrt{\frac{2}{3}} & \sqrt{\frac{2}{3}} \\ \sqrt{\frac{13}{18}} & \sqrt{\frac{13}{18}} & \sqrt{\frac{13}{18}} & \sqrt{\frac{13}{18}} & \sqrt{\frac{13}{18}} & \sqrt{\frac{13}{18}} \\ \sqrt{\frac{3}{4}} & & & & & \end{array} \right) \\ \sqrt{\frac{3}{4}} \end{pmatrix}, \quad (41)$$

while for $|\Phi_{\text{GHZ}}\rangle$, we have

$$\tilde{\nabla}_{C_{\mathcal{R}}}(\rho_{|\Phi_{\text{GHZ}}\rangle}) = \begin{pmatrix} (0) & (0) & (0) & (0) & (0) & (0) \\ \left(\begin{array}{cccc} 0 & 0 & 0 & 0 \\ 0 & 0 & 0 & 0 \\ 0 & 0 & 0 & 0 \\ 0 & 0 & 0 & 0 \end{array} \right) & \left(\begin{array}{ccc} 0 & 0 & 0 \\ 0 & 0 & 0 \\ 0 & 0 & 0 \end{array} \right) & \left(\begin{array}{cc} 0 & 0 \\ 0 & 0 \end{array} \right) & \left(\begin{array}{c} 0 \\ 0 \\ 0 \end{array} \right) \\ \left(\begin{array}{cccccc} 1 & 1 & 1 & 1 & \sqrt{\frac{2}{3}} & \sqrt{\frac{2}{3}} \\ \sqrt{\frac{8}{9}} & \sqrt{\frac{8}{9}} & \sqrt{\frac{8}{9}} & \sqrt{\frac{8}{9}} & \sqrt{\frac{8}{9}} & \sqrt{\frac{8}{9}} \end{array} \right) \\ 1 \end{pmatrix}, \quad (42)$$

showing that $|\psi_{\mathcal{W}}\rangle$ has many more sites of entanglement correlation than $|\Phi_{\text{GHZ}}\rangle$, as shown also by their unnormalized absolute ent-concurrences, $\tilde{C}_{\mathcal{R}_{\text{abs}}}(\rho_{|\psi_{\mathcal{W}}\rangle}) \approx 26.19$ and $\tilde{C}_{\mathcal{R}_{\text{abs}}}(\rho_{|\Phi_{\text{GHZ}}\rangle}) \approx 13.11$, although $|\psi_{\mathcal{W}}\rangle$ contains no mode groups that are maximally entangled (since none get up to 1, since each element *is* normalized), while $|\Phi_{\text{GHZ}}\rangle$ contains *five* maximally entangled mode groups.

However, as pointed out in [21], it is important to keep in mind that these entanglement correlations may not all be simultaneously available as resources. Rather, the ent-concurrence array shows us all *potential* entanglement resources a state has to offer. Therefore, whether we consider $|\psi_{\mathcal{W}}\rangle$ to be more or less “entangled” than $|\Phi_{\text{GHZ}}\rangle$ depends on our specific application, but the ent-concurrence array gives us a tool for assessing this.

For comparison, for $|\Phi_{\mathcal{F}}\rangle$ of (14),

$$\tilde{\nabla}_{C_{\mathcal{R}}}(\rho_{|\Phi_{\mathcal{F}}\rangle}) = \begin{pmatrix} (0) & (0) & (0) & (0) & (0) & (0.0541) \\ \left(\begin{array}{ccc} 1 & 1 & 0.0541 \\ 0.817 & & \end{array} \right) & \left(\begin{array}{cc} 1 & 1 \\ 0.817 & \end{array} \right) & \left(\begin{array}{c} 0 & 1 \\ \sqrt{\frac{2}{3}} & \sqrt{\frac{2}{3}} \end{array} \right) & \left(\begin{array}{c} 0 & 1 \\ \sqrt{\frac{2}{3}} & \sqrt{\frac{2}{3}} \end{array} \right) \\ \left(\begin{array}{cccc} 1 & 1 & 1 & 1 \\ \sqrt{\frac{8}{9}} & 1 & 1 & 1 \end{array} \right) \\ 1 \end{pmatrix}, \quad (43)$$

so that $\tilde{C}_{\mathcal{R}_{\text{abs}}}(\rho_{|\Phi_{\mathcal{F}}\rangle}) \approx 25.13$, and for $|\Phi_{\text{BP}}\rangle$ of (14),

$$\tilde{\nabla}_{C_{\mathcal{R}}}(\rho_{|\Phi_{\text{BP}}\rangle}) = \begin{pmatrix} (1) & (0) & (0) & (0) & (0) & (1) \\ \left(\begin{array}{cc} 1 & 1 \\ \sqrt{\frac{2}{3}} & \sqrt{\frac{2}{3}} \end{array} \right) & \left(\begin{array}{c} 1 & 1 \\ \sqrt{\frac{2}{3}} & \sqrt{\frac{2}{3}} \end{array} \right) & \left(\begin{array}{c} 0 & 1 \\ \sqrt{\frac{2}{3}} & \sqrt{\frac{2}{3}} \end{array} \right) & \left(\begin{array}{c} 0 & 1 \\ \sqrt{\frac{2}{3}} & \sqrt{\frac{2}{3}} \end{array} \right) \\ \left(\begin{array}{cccc} 1 & 1 & 1 & 1 \\ \sqrt{\frac{2}{3}} & 1 & 1 & 1 \end{array} \right) \\ 1 \end{pmatrix}, \quad (44)$$

so that $\tilde{C}_{\mathcal{R}_{\text{abs}}}(\rho_{|\Phi_{\text{BP}}\rangle}) \approx 25.90$. Thus, $|\Phi_{\text{BP}}\rangle$ actually has the most occurrences of maximally-entangled mode groups with 21 of them, while $|\Phi_{\mathcal{F}}\rangle$ has the next highest number at 19 of them. These two states also contain reductions that are MME states as introduced in the text after (21), and $|\Phi_{\mathcal{F}}\rangle$ and $|\Phi_{\text{BP}}\rangle$ also have some rank-4 reductions that were luckily diagonal and therefore separable by any measure. Thus, $C_{\mathcal{R}_{\text{abs}}}$ orders states *differently* than $C_{\mathcal{R}}$ due to its inclusion of the reductions.

A Possible RMS Relationship

From (41–44), in each S -mode ent-concurrence vector $\Xi_{C_Y}^{(\mathbf{m})}$, the higher-partitional elements are the root-mean-square (RMS) of 2-partitional elements with one partition of the same mode group. Thus, for the 3-mode vectors,

$$\hat{C}_Y^{(a|b|c)} = \text{rms}(\hat{C}_Y^{(a|b,c)}, \hat{C}_Y^{(b|a,c)}, \hat{C}_Y^{(c|a,b)}), \quad (45)$$

where $\text{rms}(\mathbf{x}) \equiv (\frac{1}{\dim(\mathbf{x})} \sum_{k=1}^{\dim(\mathbf{x})} |x_k|^2)^{1/2}$. For example, in (43), $\hat{C}_Y^{(1|2|3)} = [\frac{1}{3}(1^2 + 1^2 + 0.0541^2)]^{1/2} = 0.817$. For the N -mode vectors,

$$\begin{aligned} \hat{C}_Y^{(a|b|c,d)} &= \text{rms}(\hat{C}_Y^{(a|b,c,d)}, \hat{C}_Y^{(b|a,c,d)}, \hat{C}_Y^{(a,b|c,d)}), \\ \hat{C}_Y^{(1|2|3|4)} &= \text{rms}(\hat{C}_Y^{(1|2,3,4)}, \hat{C}_Y^{(2|1,3,4)}, \hat{C}_Y^{(3|1,2,4)}, \hat{C}_Y^{(4|1,2,3)}), \end{aligned} \quad (46)$$

up to irrelevant mode permutations in and of the mode groups. Since this was only tested for (41–44), it is merely a hypothetical relationship in general at this time.

VIII. CONCLUSIONS

We have explored several multipartite entanglement measures, and found that one of them called the *ent-concurrence* \hat{C}_Y of (22), can distinguish between maximally F_N -entangled states with different amounts of entanglement between all possible mode groups. Its name indicates the fact that \hat{C}_Y is exactly equal to the concurrence C for all pure and mixed states of two qubits, while for all larger systems, it is a function of *the ent* Y , a necessary and sufficient measure of F_N -entanglement in N -mode systems [21, 29].

The reason that an F_N -entanglement measure like the ent Y can be used in a multipartite entanglement measure is that since every partitioning of $T \leq N$ mode groups can be treated as a T -mode system, Y can be adapted as the *N -mode partitional ent* $Y^{(N(T))}$ to evaluate the F_T -entanglement of those T mode groups. Then, the N -mode partitional ent-concurrence $C_Y^{(N(T))}$ for each partitioning of the state is the square root of the N -mode partitional ent, and the ent-concurrence C_Y is a 1-norm over all of the N -mode partitional ent-concurrences. Mixed states are handled by the convex-roof extension (CRE) of C_Y as \hat{C}_Y (as with C , we can omit the hat).

Note that for pure and mixed states of a 2-qubit system, $(\hat{C}_Y)^2$ is exactly equal to the *tangle* from [7]. Thus, \hat{C}_Y can be thought of as the square root of a multipartite generalization of the tangle. Then, while adding up all the N -mode partitional ents yielded the occasional inability to distinguish between different kinds of F_k -entanglement for pure states, we found that the ent-concurrence C_Y did not have this problem, since it is sensitive to how the entanglement is distributed throughout ρ . Therefore, \hat{C}_Y is a more appropriate measure than $(\hat{C}_Y)^2$ as a generalization of the tangle, despite their close relationship.

While ent-concurrence C_Y is a good measure of multipartite entanglement for applications needing entanglement of the full input state ρ , we also defined the *absolute ent-concurrence* $C_{Y_{\text{abs}}}$ as a measure that additionally

takes into account the entanglement between all possible partitions of all possible *reductions* $\check{\rho}^{(\mathbf{m})}$. Thus, $C_{Y_{\text{abs}}}$ is for applications where it is important to have entanglement within the reductions as well as the full state.

The ent-concurrence array \tilde{V}_{C_Y} of (36) shows that our application really determines what kind of measure we use. One alternative not explored here is to just target a specific reduction or a group of these such as all reductions composed of three modes, and define a *modal ent-concurrence vector* and accompanying measure of *modal ent-concurrence* in analogy to the modal ent of [21]. Such measures could ignore entanglement in the full Hilbert space, focusing only on entanglement in the reductions. Since this kind of measure is very specific, it allows one to make highly customized multipartite entanglement measures suited to specific applications.

We also noted that entanglement means *nonseparable nonlocal correlation* (NSNLC), and that measures, such as “genuinely multipartite” (GM) entanglement measures, which test for the presence of *any separability*, are not sufficient to detect the absence of all NSNLC, and are thus insufficient to detect all multipartite entanglement.

However, GM entanglement measures may still have use as *k -inseparability measures*, allowing us to determine whether separability is possible between any k -mode groups. Yet we must keep in mind that just because a state is separable over a *particular* k -partition does not mean that NSNLC (and thus entanglement) do not exist between *other* k -partitions. For the purpose of *k -inseparability measures*, our proposed *strict* FGM (SFGM) of formation from (17) gives the option to only report as *k -separable* those mixed states for which every pure decomposition state is separable over the same particular mode groups, to avoid the fallacy of thinking of states such as (2) as being devoid of k -partitional NSNLC, as explained in App. H.

Another important point, made in App. B, is that true separability implies the ability to mathematically reconstruct a mixed parent state from its reductions. Therefore, if a measure reports any state as separable in some way, there must be, at least in principle, a way to find the decompositions of the relevant reduced states that can be used to exactly reconstruct the parent state. In general, GM measures do not indicate whether such reconstructions are possible, while the ent-concurrence (and a few other proposed measures) are *guaranteed* to indicate this.

While the ent-concurrence C_Y is a simple and easily computable multipartite entanglement measure for pure states, its mixed-state definition as a convex-roof extension (CRE) makes it intractable to approximate for states with rank > 2 , a difficulty common to all CRE-based measures. Therefore, an interesting avenue for future research is the search for a *computable* formula for the ent-concurrence C_Y for all mixed-state input.

We may also conjecture that different “tiers” of maximally F_N -entangled states (such as those in Sec. VI) contain enough states to make a maximally-entangled basis (MEB) set. This was proven to be always possible in [21]

for F_N -entangled states, so the tier-specific version can be considered as the “strong-MEB” theorem, and would also be interesting for future research.

Hopefully, the ent-concurrence C_Υ will enable advancements in the study of multipartite entanglement and our understanding of it.

ACKNOWLEDGMENTS

Many thanks to Ting Yu and B. D. Clader for helpful feedback and discussions.

Appendix A: Brief Review of Reduced States

We represent *multipartite state reduction* to a composite subsystem of $S \in 1, \dots, N$ potentially noncontiguous and reordered modes $\mathbf{m} \equiv (m_1, \dots, m_S)$, as

$$\check{\rho}^{(\mathbf{m})} \equiv \text{tr}_{\bar{\mathbf{m}}}(\rho), \quad (\text{A1})$$

where the “check” in $\check{\rho}^{(\mathbf{m})}$ indicates that it is a *reduction* of *parent state* ρ (and not merely an isolated system of same size as mode group \mathbf{m}), and the bar in $\bar{\mathbf{m}}$ means “not \mathbf{m} ,” telling us to trace over all modes whose labels are *not* in \mathbf{m} . See [21, App. B] for details.

Appendix B: N -Separability of N -Partite States Implies Reconstructability by Smallest Reductions

Recalling the N -separable states $\zeta^{(1, \dots, N)}$ of (3), we will show that each mode- m reduction admits a decomposition of the form $\check{\zeta}^{(m)} \equiv \sum_j p_j \check{\zeta}_j^{(m)} = \sum_j p_j \zeta_j^{(m)}$, letting us express the parent state entirely in terms of the mode- m decomposition reductions as

$$\zeta^{(1, \dots, N)} = \sum_j p_j \check{\zeta}_j^{(1)} \otimes \dots \otimes \check{\zeta}_j^{(N)}, \quad (\text{B1})$$

since $\check{\zeta}_j^{(m)} \equiv \text{tr}_{\bar{\mathbf{m}}}(\zeta_j^{(1, \dots, N)}) = \zeta_j^{(m)}$, echoing the earlier observation from Sec. I that absence of entanglement correlation implies that reductions contain enough information to fully reconstruct the parent state.

As we now prove, for all *multimode* reductions (reductions involving two or more modes), N -separability of the parent state implies that all multimode reductions are also fully separable, since they too inherit the product-form of the optimal decomposition states of the parent.

First, multipartite reductions are generally mixed, as

$$\check{\zeta}^{(\mathbf{m})} \equiv \sum_j p_j \check{\zeta}_j^{(\mathbf{m})}, \quad (\text{B2})$$

where $\mathbf{m} \equiv (m_1, \dots, m_S)$, $S \in 1, \dots, N$, and $\{p_j, \check{\zeta}_j^{(\mathbf{m})}\}$ does not assume any structural similarity to the parent state. Then, from the definition of multipartite reduction,

$$\begin{aligned} \check{\zeta}^{(\mathbf{m})} &\equiv \text{tr}_{\bar{\mathbf{m}}}(\zeta^{(1, \dots, N)}) \\ \sum_j p_j \check{\zeta}_j^{(\mathbf{m})} &= \text{tr}_{\bar{\mathbf{m}}}(\sum_j p_j \zeta_j^{(1, \dots, N)}) \\ &= \sum_j p_j \text{tr}_{\bar{\mathbf{m}}}(\zeta_j^{(1, \dots, N)}) \\ &= \sum_j p_j \text{tr}_{\bar{\mathbf{m}}}(\zeta_j^{(1)} \otimes \dots \otimes \zeta_j^{(N)}) \\ &= \sum_j p_j \zeta_j^{(m_1)} \otimes \dots \otimes \zeta_j^{(m_S)}, \end{aligned} \quad (\text{B3})$$

where we used the facts that $\text{tr}(A \otimes B) = \text{tr}(A) \otimes \text{tr}(B) = \text{tr}(A)\text{tr}(B)$ and $\text{tr}(\zeta_j^{(\bar{m}_k)}) = 1$ for normalized states $\zeta_j^{(\bar{m}_k)}$, which were applicable due to the N -separability of the parent. Setting $S = 1$ in (B3) yields our earlier result that $\check{\zeta}_j^{(m)} = \zeta_j^{(m)}$ (since for $S = 1$, $\mathbf{m} = m_1 = m$), which holds for $m \in 1, \dots, N$ and lets us rewrite (B3) as

$$\check{\zeta}^{(\mathbf{m})} = \sum_j p_j \check{\zeta}_j^{(m_1)} \otimes \dots \otimes \check{\zeta}_j^{(m_S)}, \quad (\text{B4})$$

showing that *all* multimode reductions of N -separable states are S -separable S -partite states, so they have no entanglement correlation at all, and can *all* be reconstructed by information in the *single-mode* reductions. Thus, setting $S = N$ in \mathbf{m} in (B4) proves (B1) as well.

Appendix C: Definition of Partitions

Partitioning is the act of defining *new modes*. We let the new mode structure of T partitions of multimode reduction $\check{\rho}^{(\mathbf{m})}$ be $\mathbf{m}^{(\mathbf{T})} \equiv (\mathbf{m}^{(1)} | \dots | \mathbf{m}^{(T)})$, where $T \in 1, \dots, S$ and $\mathbf{m} \equiv (m_1, \dots, m_S)$, and $S \in 1, \dots, N$, where ρ is an N -partite state, and the T new modes defined by the partitioning have internal structures $\mathbf{m}^{(q)} \equiv (m_1^{(q)}, \dots, m_G^{(q)})$ where $G \equiv G^{(q)} \in 1, \dots, S$ in terms of original indivisible modes m_k such that all m_k appear exactly once among all new mode groups $\mathbf{m}^{(q)}$.

The new mode groups have levels vector $\mathbf{n}^{(\mathbf{m}^{(\mathbf{T})})} \equiv (n_{\mathbf{m}^{(1)}}, \dots, n_{\mathbf{m}^{(T)}})$ where $n_{\mathbf{m}^{(q)}} \equiv n_{m_1^{(q)}} \dots n_{m_G^{(q)}}$. Thus we will always have the same number of levels in both $\check{\rho}^{(\mathbf{m})}$ and its partitioned version $\check{\rho}^{(\mathbf{m}^{(\mathbf{T})})}$ so that $n_{\mathbf{m}} = n_{\mathbf{m}^{(\mathbf{T})}}$, where $n_{\mathbf{m}} \equiv n_{m_1} \dots n_{m_S}$ is the number of levels of $\check{\rho}^{(\mathbf{m})}$, and $n_{\mathbf{m}^{(\mathbf{T})}} \equiv n_{\mathbf{m}^{(1)}} \dots n_{\mathbf{m}^{(T)}}$ is the number of levels of $\check{\rho}^{(\mathbf{m}^{(\mathbf{T})})}$. Sometimes we use the notation $n^{(\mathbf{m}^{(\mathbf{T})})} \equiv n_{\mathbf{m}^{(\mathbf{T})}}$ to allow space for quantities like $n_{\max}^{(\mathbf{m}^{(\mathbf{T})})}$ as in [21].

Here, the partition symbol “|” denotes our conceptual redefinition of the mode structure, so that “|” is the delimiter of the new mode list, while the commas “,” serve as secondary delimiters to be ignored with respect to separability, but shown to indicate how the old modes contribute to the new modes. In a mode list with no partitions “|”, commas “,” *are* the partitions. Note that we can never subdivide the smallest modes defining the N -partite system, since they are defined by the fundamental coincidence behavior of the system and therefore have no internal coincidences of their own (see [21, App. A]).

Also note that T is the number of mode groups *formed* by the partitions, and is always one more than the number of partition symbols “|”. For ease of speech, we will speak of “ T partitions” or describe something as “ T -partitional” when we are referring to it having T *mode groups*, and it is implied that there are always $T - 1$ conceptual partitions “|” that define these mode groups.

Appendix D: Proof that N -Partite States are Entangled If and Only If they are F_N -Partite Entangled

First, we establish some useful definitions and a theorem, then we prove necessity and sufficiency separately, in terms of separability, and finally unite the cases. See App. A and App. C for supporting explanations.

1. Definitions and Theorem

Definition 1: Let the set of all unique multimode T -partitions of all S -mode reductions of an N -partite system, where $2 \leq T \leq S \leq N$, be called *the set of all multimode T -partitions*. For example: the multimode T -partitions of $\rho^{(1,2,3)}$ are $\{\check{\rho}^{(1|2)}, \check{\rho}^{(1|3)}, \check{\rho}^{(2|3)}, \check{\rho}^{(1|2,3)}, \check{\rho}^{(2|1,3)}, \check{\rho}^{(3|1,2)}, \check{\rho}^{(1|2|3)}\}$.

Definition 2: Let the $T \geq 2$ modes of a T -partitioned state that is not T -separable (meaning it cannot be expressed as a convex sum of a tensor product of T pure states) be called *entanglement-correlated* (or *entangled*), and said to have *entanglement correlations* (or *entanglement*) because knowledge of the T single-mode reductions cannot be used to reconstruct the full T -mode state. For example, given parent $\rho \equiv \rho^{(1,2,3)}$, if $\check{\rho}^{(1|3)} \neq \sum_j p_j \rho_j^{(1)} \otimes \rho_j^{(3)}$ for some pure $\rho_j^{(1)}$ and $\rho_j^{(3)}$, then modes 1 and 3 of ρ are entanglement-correlated, so the reduction $\check{\rho}^{(1,3)} = \check{\rho}^{(1|3)}$ has entanglement correlations. (We say *entanglement correlation* instead of just *entanglement* as a reminder that there are *other* types of nonlocal correlation that do not involve entanglement.)

Theorem 1: *The set of all multimode T -partitions from Definition 1 is the set all possible mode groups that could exhibit entanglement correlations within a state.* Proof: (i) It is not possible to define any other multimode groups within the system, since the original modes cannot be subdivided (see [21, App. A]); therefore this list of mode groups is exhaustive. (ii) By Definition 2, entanglement correlations can only exist between two or more modes. (iii) Therefore, by (i) and (ii), Theorem 1 is proven.

For applications of entanglement in the full Hilbert space (not within reductions), we will use a relaxed version of Theorem 1, that only uses the set of multimode T -partitions of the full N -mode state, ignoring its reductions. See Sec. III D.

2. Proof That N -Separability Is Sufficient for Absence of All Entanglement Correlations

We already proved in (B4) that all S -mode reductions $\zeta^{(\mathbf{m})}$ of N -separable N -partite states ς are S -separable. Therefore, by Theorem 1, in order to show that all possible entanglement correlations of ς are absent, we need to show for any *partitions* of $\mathbf{m} \equiv (m_1, \dots, m_S)$ in the states of (B4) such as $\mathbf{m}' \equiv (m_1|m_2, m_3)$, that such states are *also separable across all partitions*, a fact easily proven since partitions in S -separable states only result in selectively ignoring separability between certain modes.

For an example of how T -partite partitioning of S -separable S -partite states yields T -separability, observe that 2-partition of a 3-partite 3-separable state gives $\zeta^{(\mathbf{m}')} \equiv \zeta^{(m_1|m_2, m_3)} = \sum_j p_j \zeta_j^{(m_1)} \otimes (\zeta_j^{(m_2)} \otimes \zeta_j^{(m_3)}) \equiv \sum_j p_j \zeta_j^{(m_1)} \otimes \zeta_j^{(m_2, m_3)}$, where $\zeta_j^{(m_2, m_3)} \equiv \zeta_j^{(m_2)} \otimes \zeta_j^{(m_3)}$, showing that in S -separable states, partitioning means grouping modes together and ignoring their internal separability, so *the resulting mode groups are separable with each other*, due to the underlying S -separability of $\zeta^{(\mathbf{m})}$.

For a general proof of this, let σ be a T -separable T -partitioned S -mode mixed state with the form

$$\sigma \equiv \sigma^{(\mathbf{m}^{(1)}|\dots|\mathbf{m}^{(T)})} \equiv \sum_j p_j \sigma_j^{(\mathbf{m}^{(1)})} \otimes \dots \otimes \sigma_j^{(\mathbf{m}^{(T)})}, \quad (\text{D1})$$

where $\sigma_j^{(\mathbf{m}^{(q)})}$ are new-mode- $\mathbf{m}^{(q)}$ pure states of the optimal decomposition, keeping in mind that for a given T , there is generally more than one way to partition the state to T new modes.

Then, similarly to (B3) and (B4), the $\mathbf{m}^{(\mathbf{q})}$ -mode reductions $\check{\sigma}^{(\mathbf{m}^{(\mathbf{q})})} \equiv \sum_j p_j \check{\sigma}_j^{(\mathbf{m}^{(\mathbf{q})})}$ of σ , where $\mathbf{q} \equiv (q_1, \dots, q_Q)$ and $Q \in 1, \dots, T$, are

$$\begin{aligned} \check{\sigma}^{(\mathbf{m}^{(\mathbf{q})})} &\equiv \text{tr}_{\overline{\mathbf{m}^{(\mathbf{q})}}}(\sigma^{(\mathbf{m}^{(1)}|\dots|\mathbf{m}^{(T)})}) \\ \sum_j p_j \check{\sigma}_j^{(\mathbf{m}^{(\mathbf{q})})} &= \sum_j p_j \text{tr}_{\overline{\mathbf{m}^{(\mathbf{q})}}}(\sigma_j^{(\mathbf{m}^{(1)})} \otimes \dots \otimes \sigma_j^{(\mathbf{m}^{(T)})}) \\ &= \sum_j p_j \sigma_j^{(\mathbf{m}^{(q_1)})} \otimes \dots \otimes \sigma_j^{(\mathbf{m}^{(q_Q)})}, \end{aligned} \quad (\text{D2})$$

and then, the $Q = 1$ case shows that $\check{\sigma}_j^{(\mathbf{m}^{(q)})} = \sigma_j^{(\mathbf{m}^{(q)})}$ (since then $\mathbf{q} = q_1 \equiv q$), which, put into (D2), yields

$$\check{\sigma}^{(\mathbf{m}^{(\mathbf{q})})} = \sum_j p_j \check{\sigma}_j^{(\mathbf{m}^{(q_1)})} \otimes \dots \otimes \check{\sigma}_j^{(\mathbf{m}^{(q_Q)})}, \quad (\text{D3})$$

and then the $Q = T$ case of (D3) yields the useful result

$$\check{\sigma}^{(\mathbf{m}^{(\mathbf{T})})} = \sum_j p_j \check{\sigma}_j^{(\mathbf{m}^{(1)})} \otimes \dots \otimes \check{\sigma}_j^{(\mathbf{m}^{(T)})}, \quad (\text{D4})$$

since we can choose $\mathbf{q} = (q_1, \dots, q_T) = (1, \dots, T) = \mathbf{T}$, which shows that a T -separable T -partite state σ can be fully described by information in its smallest reductions $\check{\sigma}^{(\mathbf{m}^{(\mathbf{q})})} \equiv \sum_j p_j \check{\sigma}_j^{(\mathbf{m}^{(\mathbf{q})})}$, *even if those reductions have internal mode structure* $\mathbf{m}^{(\mathbf{q})} \equiv (m_1^{(\mathbf{q})}, \dots, m_{q'}^{(\mathbf{q})})$.

Then, the key point is that since none of the original modes m_k of an N -separable N -partite state ς can be subdivided by partitions, the $\mathbf{m}^{(\mathbf{T})}$ -mode reductions of ς are guaranteed to be T -separable, as

$$\begin{aligned} \text{tr}_{\overline{\mathbf{m}^{(\mathbf{T})}}}(\varsigma) &= \text{tr}_{\overline{\mathbf{m}^{(\mathbf{T})}}}(\varsigma^{(1, \dots, N)}) \\ \check{\zeta}^{(\mathbf{m}^{(\mathbf{T})})} &= \sum_j p_j \text{tr}_{\overline{\mathbf{m}^{(\mathbf{T})}}}(\zeta_j^{(1)} \otimes \dots \otimes \zeta_j^{(N)}) \\ &= \sum_j p_j \zeta_j^{(\mathbf{m}^{(1)})} \otimes \dots \otimes \zeta_j^{(\mathbf{m}^{(T)})}, \end{aligned} \quad (\text{D5})$$

where $\zeta_j^{(\mathbf{m}^{(\mathbf{q})})} \equiv \zeta_j^{(m_1^{(\mathbf{q})})} \otimes \dots \otimes \zeta_j^{(m_{q'}^{(\mathbf{q})})}$ are pure decomposition states of $\zeta^{(\mathbf{m}^{(\mathbf{q})})}$.

Thus we have proven that if an N -partite parent state is N -separable, all of its multimode reductions to $S \in 2, \dots, N$ modes are S -separable S -partite states, and any *partitions* of any S -partite reductions of N -separable N -partite states for $S \in 2, \dots, N$, are *also separable across*

those partitions. Therefore, N -separability of N -partite states implies that there are no entanglement correlations of any kind. This yields the equivalent statements,

$$\begin{aligned} & \text{(N-separability of the full state)} \\ & \text{is sufficient for} \\ & \left(\begin{array}{l} \text{the simultaneous absence of} \\ \text{all entanglement correlations} \end{array} \right) \quad (S \Leftarrow N), \quad (\text{D6}) \end{aligned}$$

$$\begin{aligned} & \text{(F_N-entanglement of the full state)} \\ & \text{is necessary for} \\ & \left(\begin{array}{l} \text{the presence of any} \\ \text{entanglement correlations} \end{array} \right) \quad (\bar{S} \Rightarrow \bar{N}), \quad (\text{D7}) \end{aligned}$$

where S and N are labels for conditions of a conditional statement where we chose N to represent “ N -separability of the full state” and S to represent “the simultaneous absence of all entanglement correlations,” and the phrase “the full state” means “the full N -partite parent state.”

3. Proof That N -Separability Is Necessary for Absence of All Entanglement Correlations

Here, the claim we want to test is

$$\begin{aligned} & \text{(N-separability of the full state)} \\ & \text{is necessary for} \\ & \left(\begin{array}{l} \text{the simultaneous absence of} \\ \text{all entanglement correlations} \end{array} \right) \quad (S \Rightarrow N). \quad (\text{D8}) \end{aligned}$$

To prove (D8), suppose that N -separability is *not* necessary for the simultaneous absence of all entanglement correlations. Then, that means there could exist states ϱ that could be F_N -entangled, and yet *also* have simultaneous absence of all entanglement correlations. Therefore, the F_N -entanglement of such states would mean that

$$\varrho^{(1,\dots,N)} \neq \sum_j p_j \check{\varrho}_j^{(1)} \otimes \dots \otimes \check{\varrho}_j^{(N)}, \quad (\text{D9})$$

while their simultaneous absence of all entanglement correlations means that all of their T -partitioned S -mode reductions must be T -separable, so that, as proved in (D5),

$$\check{\varrho}^{(\mathbf{m}^{(T)})} = \sum_j p_j \check{\varrho}_j^{(\mathbf{m}^{(1)})} \otimes \dots \otimes \check{\varrho}_j^{(\mathbf{m}^{(T)})}, \quad (\text{D10})$$

for all $2 \leq T \leq S$ and $2 \leq S \leq N$, where S is the number of modes of a reduction without the partitions. Then, computing all T -partitioned S -mode reductions of (D9) by taking the partial trace gives

$$\text{tr}_{\overline{\mathbf{m}^{(T)}}}(\varrho^{(1,\dots,N)}) \neq \sum_j p_j \check{\varrho}_j^{(\mathbf{m}^{(1)})} \otimes \dots \otimes \check{\varrho}_j^{(\mathbf{m}^{(T)})}, \quad (\text{D11})$$

but since $\check{\varrho}^{(\mathbf{m}^{(T)})} \equiv \text{tr}_{\overline{\mathbf{m}^{(T)}}}(\varrho^{(1,\dots,N)})$ by definition, then we can put (D10) into the left side of (D11) to get

$$\sum_j p_j \check{\varrho}_j^{(\mathbf{m}^{(1)})} \otimes \dots \otimes \check{\varrho}_j^{(\mathbf{m}^{(T)})} \neq \sum_j p_j \check{\varrho}_j^{(\mathbf{m}^{(1)})} \otimes \dots \otimes \check{\varrho}_j^{(\mathbf{m}^{(T)})}, \quad (\text{D12})$$

which is a *false statement*, meaning that the supposition is false. Thus, the statement in (D8) is *true*, and we can extract from it the corresponding statement that

$$\begin{aligned} & \text{(F_N-entanglement of the full state)} \\ & \text{is sufficient for} \\ & \left(\begin{array}{l} \text{the presence of any} \\ \text{entanglement correlations} \end{array} \right) \quad (\bar{S} \Leftarrow \bar{N}). \quad (\text{D13}) \end{aligned}$$

4. Unification of Results

Together, true statements (D6) and (D8) yield

$$\begin{aligned} & \text{(N-separability of the full state)} \\ & \text{is necessary and sufficient for} \\ & \left(\begin{array}{l} \text{the simultaneous absence of} \\ \text{all entanglement correlations} \end{array} \right) \quad (S \Leftrightarrow N), \quad (\text{D14}) \end{aligned}$$

which means we also have

$$\begin{aligned} & \text{(F_N-entanglement of the full state)} \\ & \text{is necessary and sufficient for} \\ & \left(\begin{array}{l} \text{the presence of any} \\ \text{entanglement correlations} \end{array} \right) \quad (\bar{S} \Leftrightarrow \bar{N}). \quad (\text{D15}) \end{aligned}$$

Thus, we have proven that F_N -entanglement measures are necessary and sufficient for detecting the presence of any entanglement correlations in an N -partite quantum state.

Appendix E: Normalization Factor of the Ent

Given the parameters from (5), the ent’s automatic normalization (needing no calibration state) function is

$$M(L) \equiv M(L, \mathbf{n}) \equiv 1 - \frac{1}{N} \sum_{m=1}^N \frac{n_m P_{\text{MP}}^{(m)}(L) - 1}{n_m - 1}, \quad (\text{E1})$$

where $N \equiv \dim(\mathbf{n})$ and the mode- m purity-minimizing function $P_{\text{MP}}^{(m)}(L) \equiv P_{\text{MP}}^{(m)}(L, \mathbf{n})$ is

$$\begin{aligned} P_{\text{MP}}^{(m)}(L, \mathbf{n}) \equiv & \text{mod}(L, n_m) \left(\frac{1 + \text{floor}(L/n_m)}{L} \right)^2 \\ & + (n_m - \text{mod}(L, n_m)) \left(\frac{\text{floor}(L/n_m)}{L} \right)^2, \quad (\text{E2}) \end{aligned}$$

where $\text{mod}(a, b) \equiv a - \text{floor}(\frac{a}{b})b$. The minimum physical purity of $\check{\varrho}^{(m)}$ is then $P_{\text{MP}}^{(m)}(L_*)$, where $L_* \equiv L_*(\mathbf{n})$ is any number of levels of equal nonzero probabilities that can support maximal F_N -entanglement, given by

$$\{L_*\} \equiv \{L\} \text{ s.t. } \min_{L \in 2, \dots, n_{\text{max}}} (1 - M(L)), \quad (\text{E3})$$

where $n_{\text{max}} \equiv \frac{n}{n_{\text{max}}}$ is the product of all n_m *except* n_{max} , where $n_{\text{max}} \equiv \max(\mathbf{n})$, $\mathbf{n} \equiv (n_1, \dots, n_N)$ and $n \equiv n_1 \dots n_N$. Thus, $M(L_*)$ is the factor in (5). See [21] for details. For N -qudit systems ($n_m = d \forall m$), $M(L_*) = 1$.

Appendix F: True-Generalized X (TGX) States

Explained further in [21, App. D], and first presented in [25], true-generalized X (TGX) states are a special family of density matrices that are conjectured to be related to all general states (pure and mixed) by an entanglement-preserving unitary (EPU) transformation such that the general state and the TGX state have the same entanglement, a property called *EPU equivalence*.

Restricting ourselves to F_N -entanglement, the most likely candidate for TGX states are *simple* states, defined as those for which all of the off-diagonal parent-state matrix elements appearing in the off-diagonals of the N single-mode reductions are identically zero.

For example, in 2×2 , the TGX states are X states,

$$\rho = \begin{pmatrix} \rho_{1,1} & \cdot & \cdot & \rho_{1,4} \\ \cdot & \rho_{2,2} & \rho_{2,3} & \cdot \\ \cdot & \rho_{3,2} & \rho_{3,3} & \cdot \\ \rho_{4,1} & \cdot & \cdot & \rho_{4,4} \end{pmatrix}, \quad (\text{F1})$$

where dots are zeros, while in 2×3 , the TGX states are

$$\rho = \begin{pmatrix} \rho_{1,1} & \cdot & \cdot & \cdot & \rho_{1,5} & \rho_{1,6} \\ \cdot & \rho_{2,2} & \cdot & \rho_{2,4} & \cdot & \rho_{2,6} \\ \cdot & \cdot & \rho_{3,3} & \rho_{3,4} & \rho_{3,5} & \cdot \\ \cdot & \rho_{4,2} & \rho_{4,3} & \rho_{4,4} & \cdot & \cdot \\ \rho_{5,1} & \cdot & \rho_{5,3} & \cdot & \rho_{5,5} & \cdot \\ \rho_{6,1} & \rho_{6,2} & \cdot & \cdot & \cdot & \rho_{6,6} \end{pmatrix}, \quad (\text{F2})$$

see [21, App. D] to see how these were obtained. Thus, (F2) shows that TGX states are not always X states, and [25] gave numerical evidence that (F2) can reach values of entanglement for certain rank and purity combinations not accessible to X states, which was later proven in [30], and proves that X states *cannot* exhibit EPU equivalence in general (though they can in some systems), while numerical evidence in both [25] and [30] indicates that TGX states *may* indeed have EPU equivalence in 2×3 systems. Furthermore, the conjecture of EPU equivalence from [25] was proven for the 2×2 case in [31].

In larger multipartite systems, this definition of TGX states from [25] led to the discovery of a set of TGX states that were proven in [21] to be maximally F_N -entangled, and also led to the proof of the existence of maximally entangled basis (MEB) sets in [21], first conjectured in [25]. Thus, the TGX states contain enough maximally F_N -entangled states to form a complete basis in every multipartite system.

Therefore, while the exact form of TGX states is still unproven with respect to their defining property of EPU equivalence, the hypothesis that they are *simple* states as defined above has been shown to be consistent with EPU equivalence in many numerical and analytical tests.

Appendix G: Full Set of 4-Qubit Maximally F_N -Entangled TGX States Involving $|1\rangle$

From [21], the 13-step algorithm yields the full set of 4-qubit maximally F_N -entangled TGX states involving $|1\rangle$, with level-label convention $\{|1\rangle, |2\rangle, \dots, |16\rangle\} \equiv \{|1,1,1,1\rangle, |1,1,1,2\rangle, \dots, |2,2,2,2\rangle\}$, as

$$|\Phi_j^{[L_*]}\rangle \equiv \frac{1}{\sqrt{L_*}} \sum_{k=1}^{L_*} |(L_{\text{ME}}^{[L_*]})_{j,k}\rangle, \quad (\text{G1})$$

where L_* is the number of *nonzero levels* (nonzero probability amplitudes of these states), and $L_{\text{ME}}^{[L_*]}$ is the matrix of generic-basis-level labels for a given L_* , given by

$$L_{\text{ME}}^{[2]} = \begin{pmatrix} 1 & 16 \end{pmatrix}, \quad L_{\text{ME}}^{[4]} = \begin{pmatrix} 1 & 4 & 13 & 16 \\ 1 & 4 & 14 & 15 \\ 1 & 6 & 11 & 16 \\ 1 & 6 & 12 & 15 \\ 1 & 7 & 10 & 16 \\ 1 & 7 & 12 & 14 \\ 1 & 8 & 10 & 15 \\ 1 & 8 & 11 & 14 \\ 1 & 8 & 12 & 13 \end{pmatrix}, \quad (\text{G2})$$

for $L_* = 2$ and $L_* = 4$, while for $L_* = 6$ and $L_* = 8$,

$$L_{\text{ME}}^{[6]} = \begin{pmatrix} 1 & 4 & 6 & 11 & 13 & 16 \\ 1 & 4 & 7 & 10 & 13 & 16 \\ 1 & 6 & 7 & 10 & 11 & 16 \end{pmatrix}, \quad (\text{G3})$$

$$L_{\text{ME}}^{[8]} = \begin{pmatrix} 1 & 4 & 6 & 7 & 10 & 11 & 13 & 16 \end{pmatrix}.$$

In (14), $|\Phi_{\text{GHZ}}\rangle \equiv |\Phi_1^{[2]}\rangle$, $|\Phi_{\text{BP}}\rangle \equiv |\Phi_1^{[4]}\rangle$, and $|\Phi_{\text{F}}\rangle \equiv |\Phi_2^{[4]}\rangle$. We show these both to show what was used in our tests, and because any tests of new measures for four qubits would benefit from starting with this set as well.

Appendix H: Quantum Mixed States Cannot Be Treated as Time-Averages of Varying Pure States

The reason that states such as (2) are considered biseparable is that “they can be prepared through a statistical mixture of bipartite [and biseparable] entangled states” [4, 6]. However, we must be careful not to think of such states as *separable*; while it is true that making a step function of the different biseparable pure states of that decomposition could yield identical tomographic results to an actual quantum mixed state of the same form, a mixture obtained from a time-average of a step function of pure states (as the term “prepare” may suggest to some) is merely an *estimation* resulting from the measurer’s ignorance about which measurements correspond to which pure states of the system’s pure-state step function.

To see why a quantum mixed state cannot be a step function of pure states, suppose we have 2-qubit pure state $|\psi\rangle \equiv a_1|1\rangle + a_2|2\rangle + a_3|3\rangle + a_4|4\rangle$, where $|1\rangle \equiv |1,1\rangle$, $|2\rangle \equiv |1,2\rangle$, etc., and $\sum_{k=1}^4 |a_k|^2 = 1$, where

$$a_k \equiv \langle k|\psi\rangle \quad (\text{H1})$$

are *wave-function overlaps* between pure quantum states $|\psi\rangle$ and $|k\rangle$. The density matrix of $|\psi\rangle$ then has elements $\rho_{y,z} \equiv \langle y|\psi\rangle\langle\psi|z\rangle = a_y a_z^*$, so its mode-1 reduction is

$$\check{\rho}^{(1)} = \begin{pmatrix} \rho_{1,1} + \rho_{2,2} & \rho_{1,3} + \rho_{2,4} \\ \rho_{3,1} + \rho_{4,2} & \rho_{3,3} + \rho_{4,4} \end{pmatrix} = \begin{pmatrix} a_1 a_1^* + a_2 a_2^* & a_1 a_3^* + a_2 a_4^* \\ a_3 a_1^* + a_4 a_2^* & a_3 a_3^* + a_4 a_4^* \end{pmatrix}, \quad (\text{H2})$$

which is *entirely* a function of the pure quantum wave function overlaps in (H1), so it is a true *quantum mixture*.

In contrast, if we tried to create (H2) from a *time-average of a pure-state step function*, the decomposition states could still contain wave-function overlaps, but the *mixture probabilities would be estimators of the classical probability that the system was actually in each particular pure quantum state*.

Therefore, we cannot truly prepare a system in the state of (2) as a time-averaged mixture, because the system would just be in different separable pure states at different times; a time-dependent *pure state*. *In principle* (whether practical or not), one could guess how to assign measurements into subsets of the tomographic estimators to the pure state of the system at the exact time of measurement, and therefore determine the exact step function of the time-dependent pure state of preparation.

The *quantum mixture* of (2) is different because its

mixture probabilities inherit the *instantaneous* nature of some pure parent state's superposition, since each is entirely a function of pure wave-function overlaps, as in (H2).

Of course, we could simply *purify* (2) and create that purified state in some larger system, and by focusing on the correct subsystem, we would then have prepared (2) as a true quantum mixture, but it would then *not* be a *time-averaged* mixture, and we could not claim it to have any true separability at any one time.

Note that even *diagonal* quantum mixtures depend entirely on wave-function overlaps. For example, if $|\psi\rangle = \frac{1}{\sqrt{2}}(|1\rangle + |4\rangle)$, which is a Bell state so that $a_1 = a_4 = \frac{1}{\sqrt{2}}$ and $a_2 = a_3 = 0$, then (H2) would become

$$\check{\rho}^{(1)} = \begin{pmatrix} a_1 a_1^* & 0 \\ 0 & a_4 a_4^* \end{pmatrix} = \begin{pmatrix} \frac{1}{2} & 0 \\ 0 & \frac{1}{2} \end{pmatrix}, \quad (\text{H3})$$

which still depends only on the pure-state probability amplitudes of its pure parent state $|\psi\rangle$.

Thus, even though states like (2) have optimal decompositions into convex sums of pure product states, *that is not indicative of the absence of entanglement*, because those decomposition states are not k -separable over the same k -partitions, and furthermore, the full state cannot be treated as instantaneously separable (meaning that it is never momentarily equal to one of its biseparable decomposition states).

-
- [1] A. Einstein, B. Podolsky, and N. Rosen, Phys. Rev. **47**, 777 (1935).
[2] E. Schrödinger, Naturwiss. **23**, 807 (1935).
[3] P. A. M. Dirac, Proc. Roy. Soc. A **114**, 243 (1927).
[4] M. Huber, H. Schimpf, A. Gabriel, C. Spengler, D. Bruß, and B. Hiesmayr, Phys. Rev. A **83**, 022328 (2011).
[5] Z. Ma, Z. Chen, J. Chen, C. Spengler, A. Gabriel, and M. Huber, Phys. Rev. A **83**, 062325 (2011).
[6] M. Huber, F. Mintert, A. Gabriel, and B. C. Hiesmayr, Phys. Rev. Lett. **104**, 210501 (2010).
[7] V. Coffman, J. Kundu, and W. K. Wootters, Phys. Rev. A **61**, 052306 (2000).
[8] M. Horodecki, P. Horodecki, and R. Horodecki, Phys. Lett. A **283**, 1 (2001).
[9] M. B. Plenio and V. Vedral, J. Phys. A **34**, 6997 (2001).
[10] J. Eisert and H. J. Briegel, Phys. Rev. A **64**, 022306 (2001).
[11] D. A. Meyer and N. R. Wallach, J. Math. Phys. **43**, 4273 (2002).
[12] M. Seevinck and G. Svetlichny, Phys. Rev. Lett. **89**, 060401 (2002).
[13] A. Miyake, Phys. Rev. A **67**, 012108 (2003).
[14] P. Wocjan and M. Horodecki, Open Syst. Inf. Dyn. **12**, 331 (2005).
[15] C. S. Yu and H. S. Song, Phys. Rev. A **72**, 022333 (2005).
[16] R. Lohmayer, A. Osterloh, J. Siewert, and A. Uhlmann, Phys. Rev. Lett. **97**, 260502 (2006).
[17] A. S. M. Hassan and P. S. Joag, Quant. Inf. Comp. **8**, 0773 (2008).
[18] D. M. Greenberger, M. Horne, and A. Zeilinger, *Bell's Theorem, Quantum Theory, and Conceptions of the Universe*, edited by M. Kafatos (Kluwer, Dordrecht, 1989).
[19] D. M. Greenberger, M. Horne, A. Shimony, and A. Zeilinger, Am. J. Phys. **58**, 1131 (1990).
[20] N. D. Mermin, Phys. Today **43**, 9 (1990).
[21] S. R. Hedemann, (2016), arXiv:1611.03882.
[22] S. Hill and W. K. Wootters, Phys. Rev. Lett. **78**, 5022 (1997).
[23] W. K. Wootters, Phys. Rev. Lett. **80**, 2245 (1998).
[24] W. Dür, G. Vidal, and J. I. Cirac, Phys. Rev. A **62**, 062314 (2000).
[25] S. R. Hedemann, (2013), arXiv:1310.7038.
[26] D. Cavalcanti, F. G. S. L. Brandão, and M. O. T. Cunha, Phys. Rev. A **72**, 040303(R) (2005).
[27] Z. G. Li, M. J. Zhao, S. M. Fei, H. Fan, and W. M. Liu, Quant. Inf. Comp. **12**, 63 (2012).
[28] A. Streltsov, H. Kampermann, and D. Bru, New. J. Phys. **12**, 123004 (2010).
[29] S. R. Hedemann, *Hyperspherical Bloch Vectors with Applications to Entanglement and Quantum State Tomography*, Ph.D. thesis, Stevens Institute of Technology (2014), UMI Diss. Pub. 3636036.
[30] P. E. M. F. Mendonça, M. A. Marchioli, and S. R. Hedemann, Phys. Rev. A **95**, 022324 (2017), arXiv:1612.01214.
[31] P. E. M. F. Mendonça, M. A. Marchioli, and D. Galetti, Ann. Phys. **351**, 79 (2014).